Supplemental Information

Comparative metabolomics reveals endogenous ligands of DAF-12, a nuclear hormone receptor regulating *C. elegans* development and lifespan

Parag Mahanti,[1,6] Neelanjan Bose,[1,6] Axel Bethke,[1] Joshua C. Judkins,[1] Joshua Wollam,[2] Kathleen J. Dumas,[3] Anna M. Zimmerman,[1] Sydney L. Campbell,[1] Patrick J. Hu,[3,4] Adam Antebi,[2,5] Frank C. Schroeder[1]*

[1]Boyce Thompson Institute and Department of Chemistry and Chemical Biology, Cornell University, Ithaca, NY 14853, USA

[2]Max Planck Institute for Biology of Ageing, Joseph Stelzmann Str. 9b, D-50931 Cologne, Germany

[3]Life Sciences Institute, University of Michigan

[4]Departments of Internal Medicine and Cell and Developmental Biology, University of Michigan Medical School, Ann Arbor, MI 48109, USA

[5]Huffington Center on Aging, Dept of Molecular and Cellular Biology, Baylor College of Medicine, One Baylor Plaza, Houston, TX 77030, USA

[6]These authors contributed equally to this work.

*Correspondence: schroeder@cornell.edu (F.C.S)

Table of Contents

SUPPLEMENTAL FIGURES

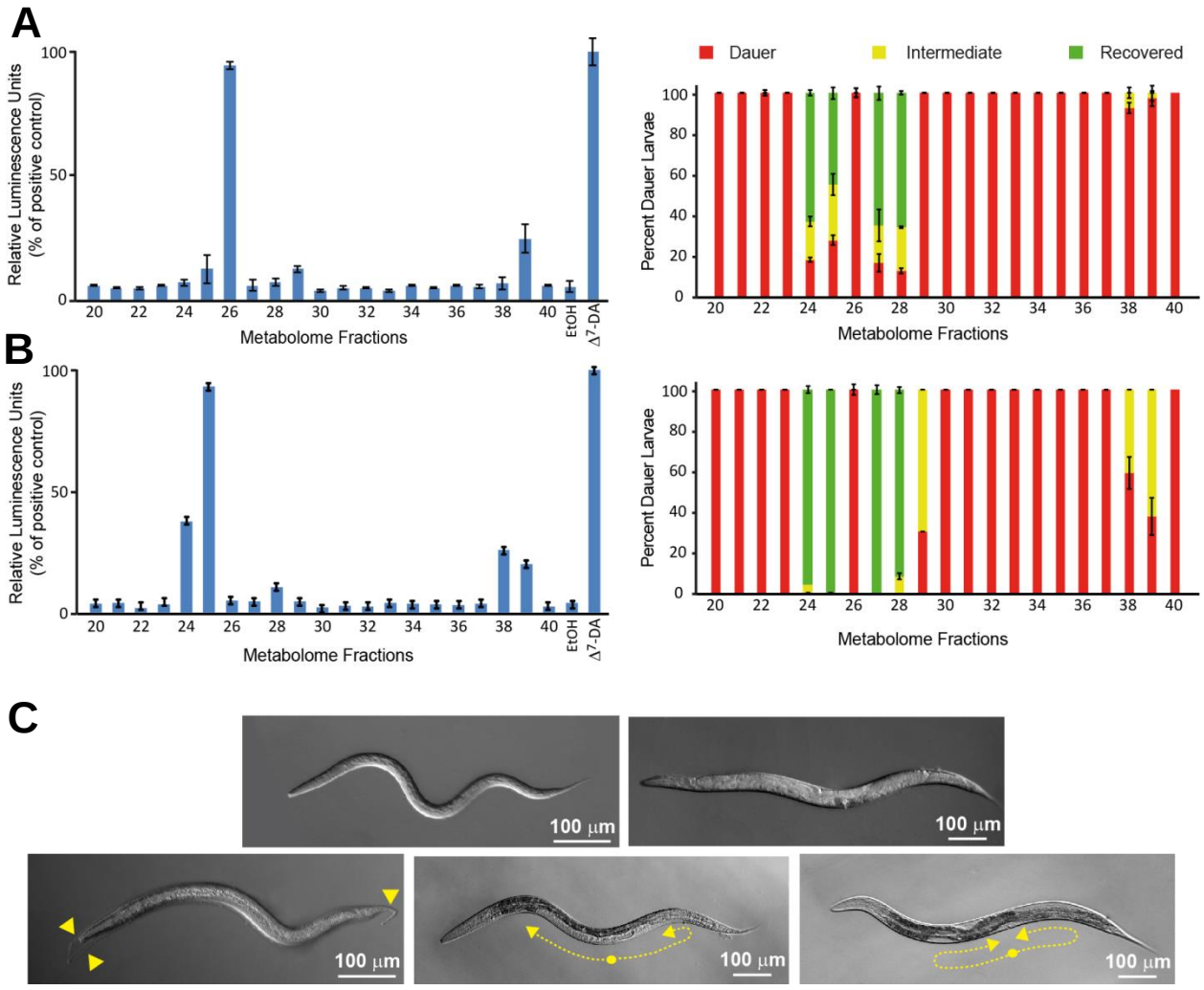

Figure S1, related to Figure 2. Bioactivity of metabolome fractions from wild type (N2) and *daf-22* mutant worms. Assessment of DAF-12 transcriptional activation in the *in vitro* luciferase assay in HEK-293T cells (left) and dauer rescue activity in *daf-9(dh6)* worms (right) with metabolome fractions obtained from **(A)** wild type **(B)** *daf-22* animals. The data show that *daf-9(dh6)* dauer rescue activity is generally higher in *daf-22* mutant metabolome fractions. For the *in vitro* luciferase assay 100 nM Δ^7-DA was used as a positive control (error bars, ±SD). **(C)** DIC images of *daf-9(dh6)* worms showing different phenotypes scored in the dauer rescue assay. Dauer (top left), adult recovered (top right), intermediate phenotypes showing molting defects (bottom left, arrows point to incompletely shed cuticle from previous molt), fully recovered late L4 (bottom center), and intermediate phenotypes showing incomplete gonad migration (bottom right). Yellow lines indicate gonadal shape in shown Mig phenotypes.

A

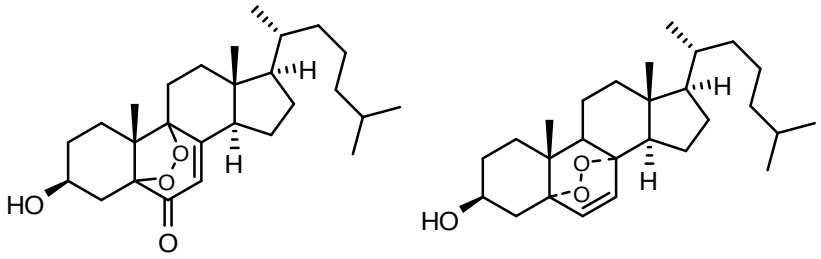

Figure S2, related to Figure 3. Identification of *C. elegans* cholesterol metabolites via DANS and SIM-GC/MS. (A) Structures of major epidioxy sterol derivatives that co-elute with Δ^7 and $\Delta^{1,7}$-DAs in active wildtype and *daf-22* mutant fractions but can also be observed in corresponding inactive *daf-9;daf-12* fractions (Gunatilaka et al., 1981; Yaoita et al., 1998).

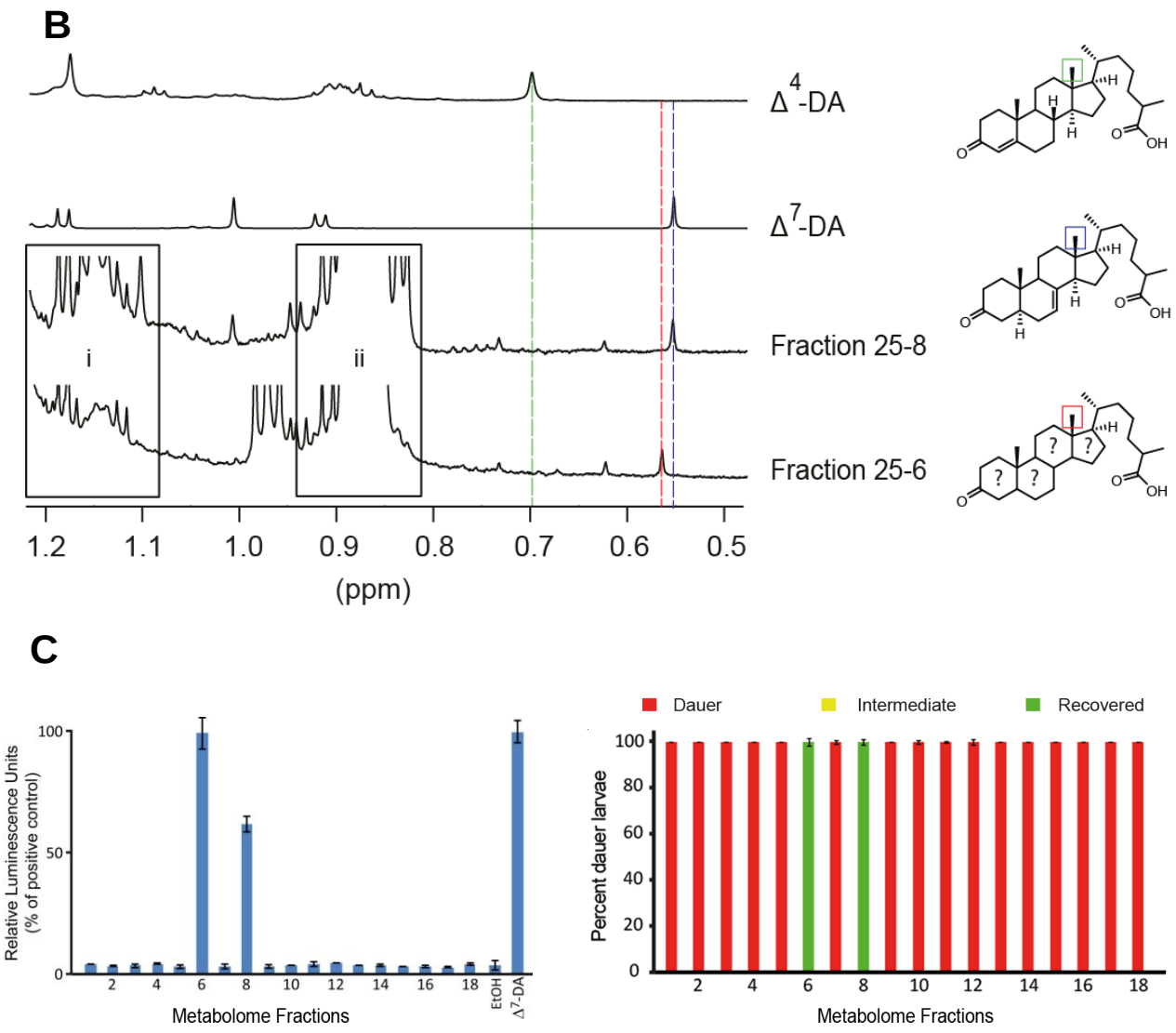

Figure S2, related to Figure 3. Identification of *C. elegans* cholesterol metabolites via DANS and SIM-GC/MS. (B) Comparison of representative sections of ^{1}H-NMR spectra of active HPLC-enriched fractions with the proposed DAF-12 ligands (Motola et al., 2006) revealed the presence of Δ^{7}-DA in fraction 25-8, and an unknown steroid ligand in fraction 25-6 that is distinctly different from Δ^{7}- and Δ^{4}-DA. ^{1}H NMR spectra of the natural fractions also show that *C. elegans* derived lipids (i, ii) constitutes the majority of the active fractions. **(C)** Assessment of DAF-12 transcriptional activation in the *in vitro* luciferase assay in HEK-293T cells (left) and dauer rescue activity in *daf-9(dh6)* worms (right) with HPLC-enriched fractions 25-6 and 25-8 obtained from *daf-22* active metabolome fraction 25. For the *in vitro* luciferase assay 100 nM Δ^{7}-DA was used as a positive control (error bars, ±SD).

D

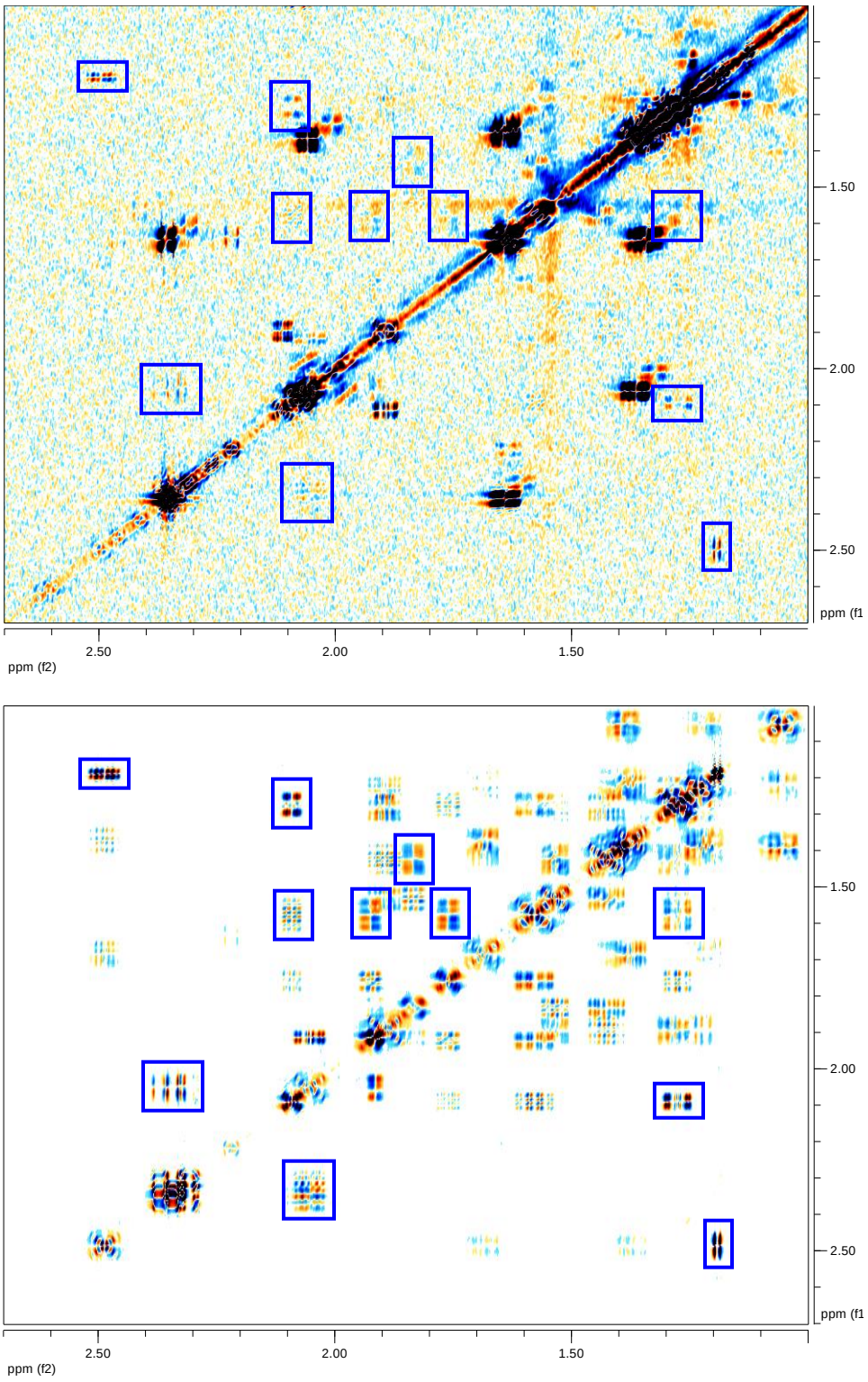

Figure S2, related to Figure 3. Identification of *C. elegans* cholesterol metabolites via DANS and SIM-GC/MS. (D) Section of dqfCOSY spectrum (600 MHz, $CDCl_3$) of *daf-22* metabolome HPLC fraction 25-6 (top). Crosspeaks indicating the presence of $\Delta^{1,7}$-DA are boxed blue. Corresponding section of the spectrum of synthetic $\Delta^{1,7}$-DA (bottom).

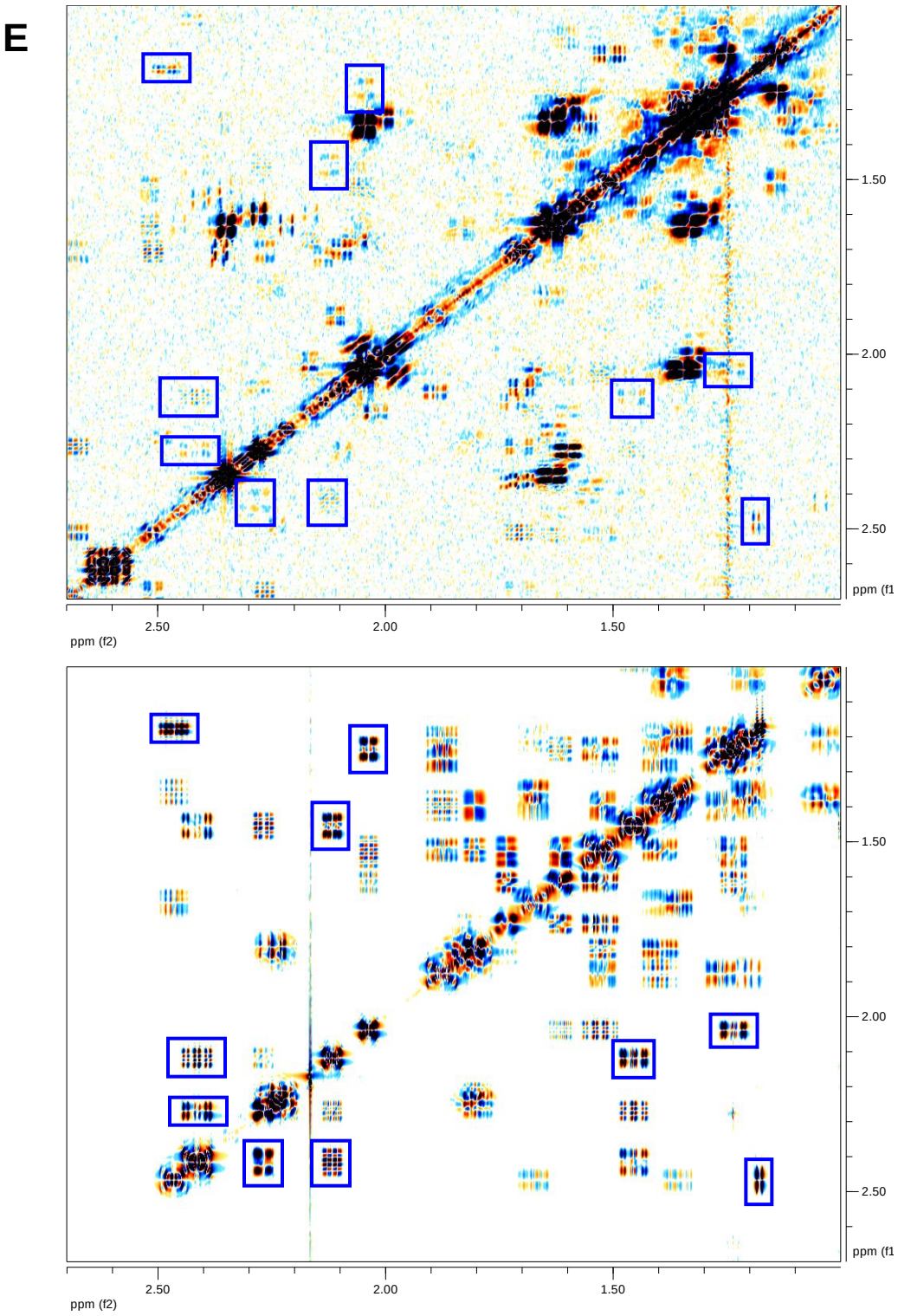

Figure S2, related to Figure 3. Identification of *C. elegans* cholesterol metabolites via DANS and SIM-GC/MS. (F)Section of dqfCOSY spectrum (600 MHz, $CDCl_3$) of HPLC fraction 25-8 from *daf-22* mutant worms (top). Characteristic crosspeaks indicating the presence of Δ^7-DA are boxed blue. Corresponding section of the spectrum of synthetic Δ^7-DA (bottom).

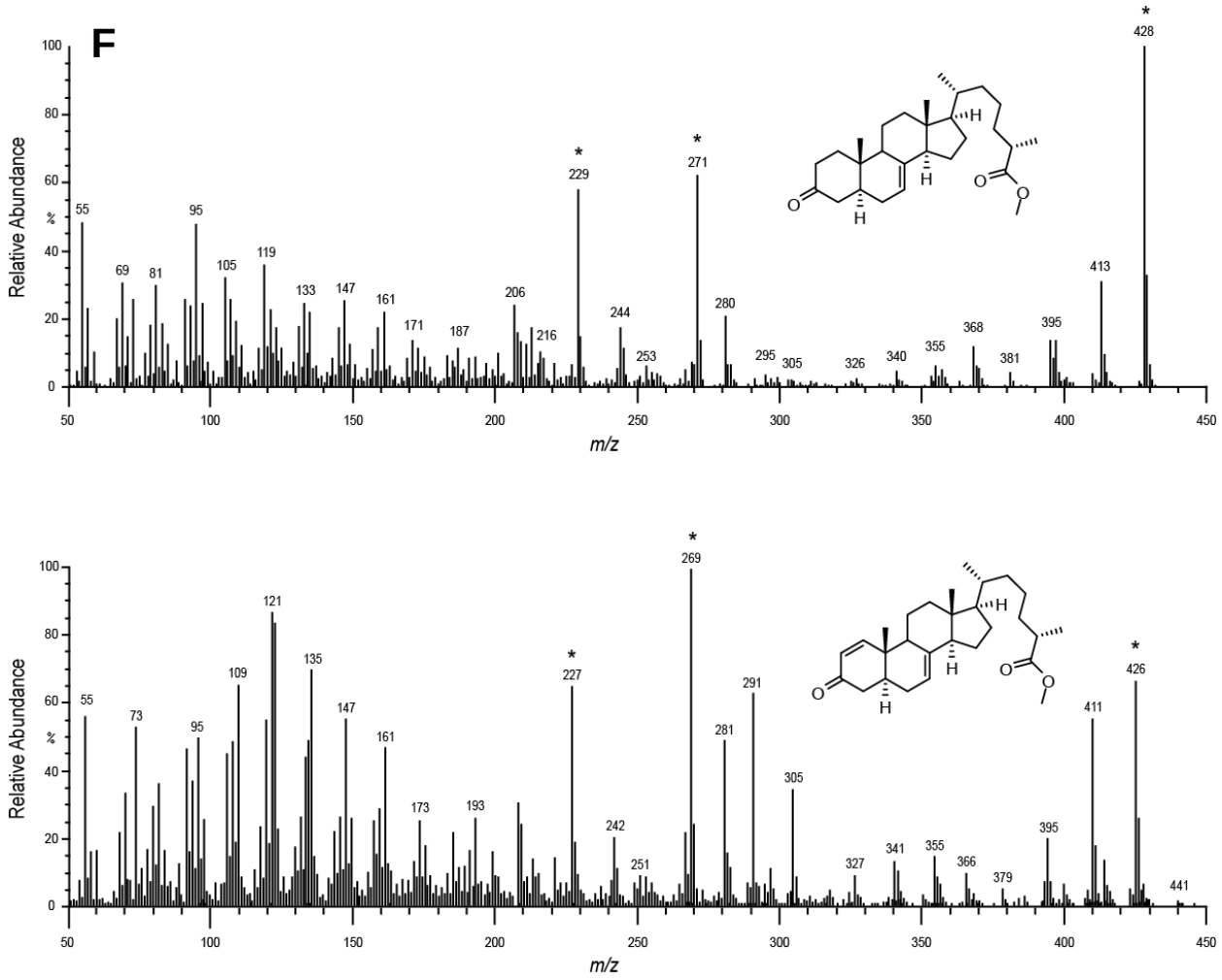

Figure S2, related to Figure 3. Identification of *C. elegans* cholesterol metabolites via DANS and SIM-GC/MS. (F) Electron-impact ionization (EI) mass spectra of methyl esters of Δ^7-DA (top) and $\Delta^{1,7}$-DA (bottom). (*) Indicates the ion fragments subsequently used for SIM-GC/MS analyses of these compounds in metabolome fractions.

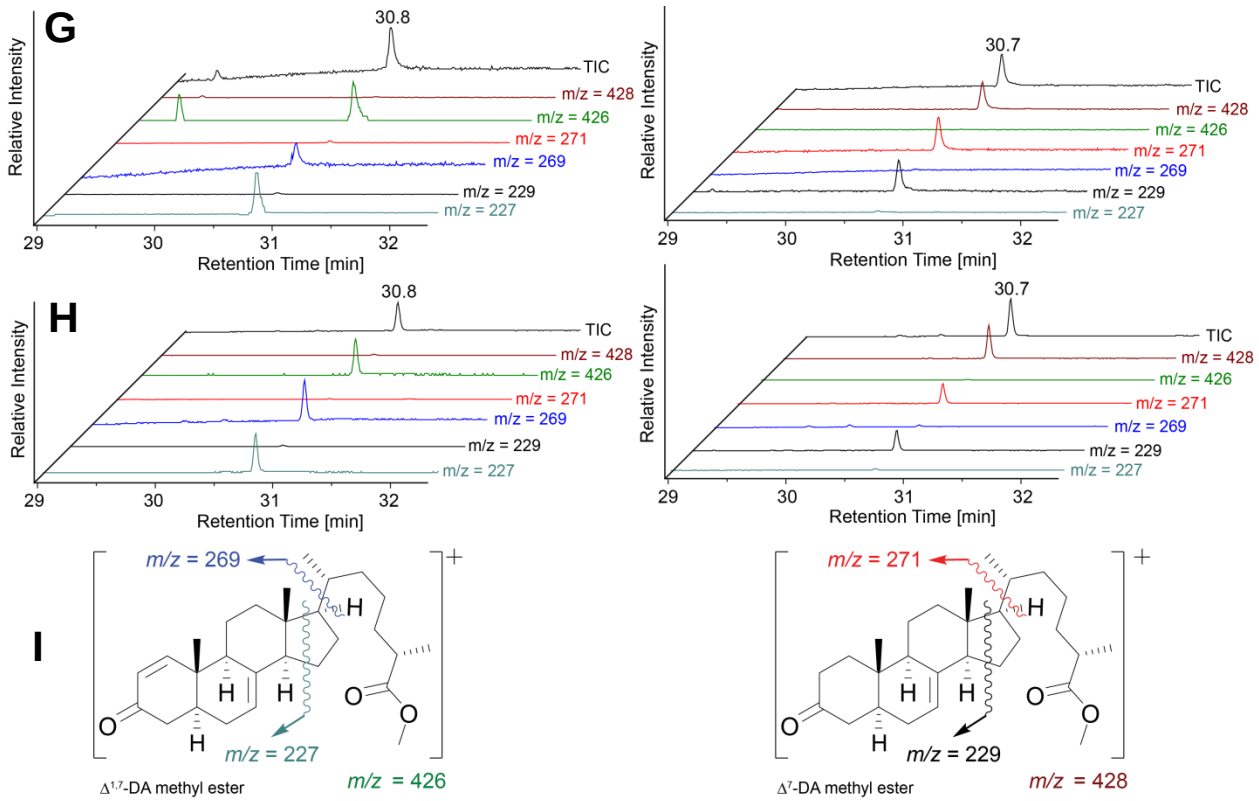

Figure S2, related to Figure 3. Identification of *C. elegans* cholesterol metabolites via DANS and SIM-GC/MS. (G) Ion chromatograms from SIM-GC/MS analysis of *daf-22* metabolome HPLC fractions 25-6 (left) and 25-8 (right), showing peaks corresponding to the methyl esters of $\Delta^{1,7}$-DA (left) and Δ^{7}-DA (right). **(H)** Corresponding chromtograms from SIM-GC/MS analysis of the methyl esters of synthetic $\Delta^{1,7}$-DA (left), and synthetic Δ^{7}-DA (right). **(I)** EI-MS fragmentation patterns of $\Delta^{1,7}$-DA methyl ester (left) and Δ^{7}-DA methyl ester (right).

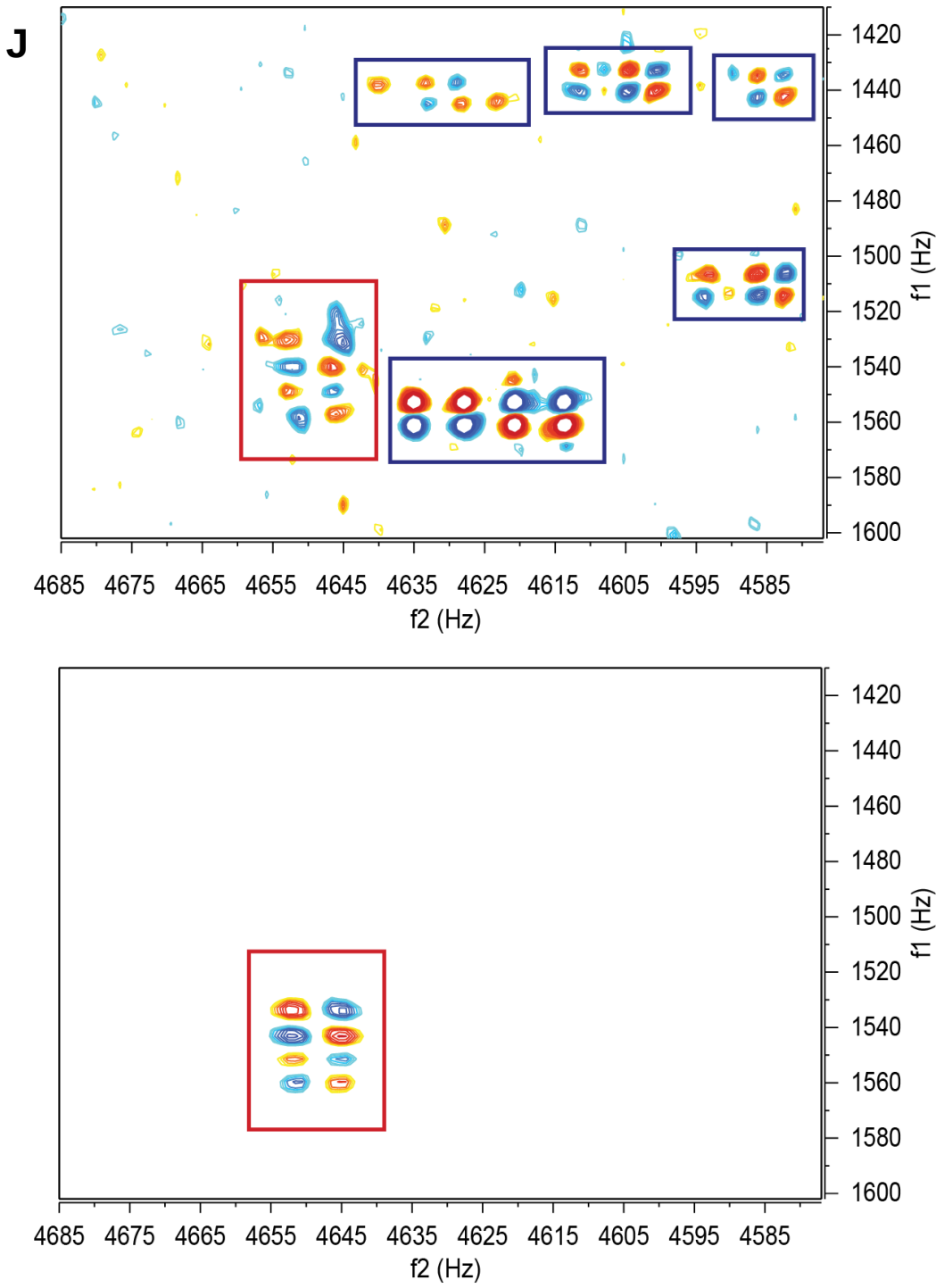

Figure S2, related to Figure 3. Identification of *C. elegans* cholesterol metabolites via DANS and SIM-GC/MS. (J) Section of dqfCOSY spectrum (900 MHz, $CDCl_3$) indicating the presence of 3α-OH- Δ^7-DA in HPLC-enriched fraction of active region II (top). Crosspeaks representing 3α-OH-Δ^7-DA are boxed red; signals from other metabolites are boxed blue. Corresponding section of dqfCOSY spectrum (600 MHz, $CDCl_3$) of synthetic 3α-OH-Δ^7-DA (bottom).

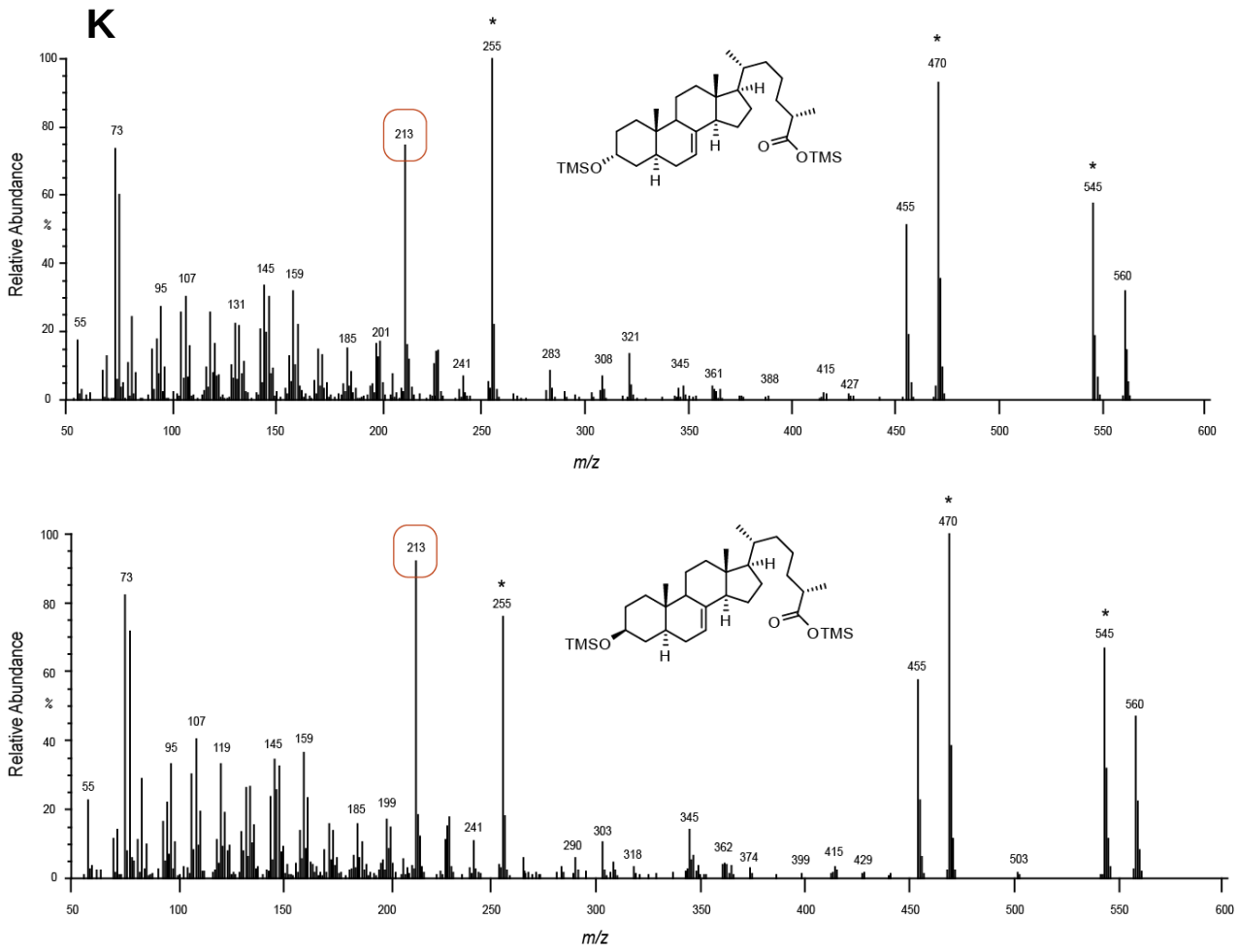

Figure S2, related to Figure 3. Identification of *C. elegans* cholesterol metabolites via DANS and SIM-GC/MS. (K) EI-MS spectum of the trimethylsilyl-derivative of synthetic 3α-OH-Δ^7-DA (top). EI-MS spectum of the TMS-derivative of synthetic 3β-OH-Δ^7-DA (bottom). (*) Indicates the fragment ions subsequently used for SIM-GC/MS-based identification of these compounds in natural samples. The red boxes highlight the fragment ion *m/z* = 213 which has been implicated in a previous publication (Held et al., 2006) as belonging to a putative DAF-12 ligand.

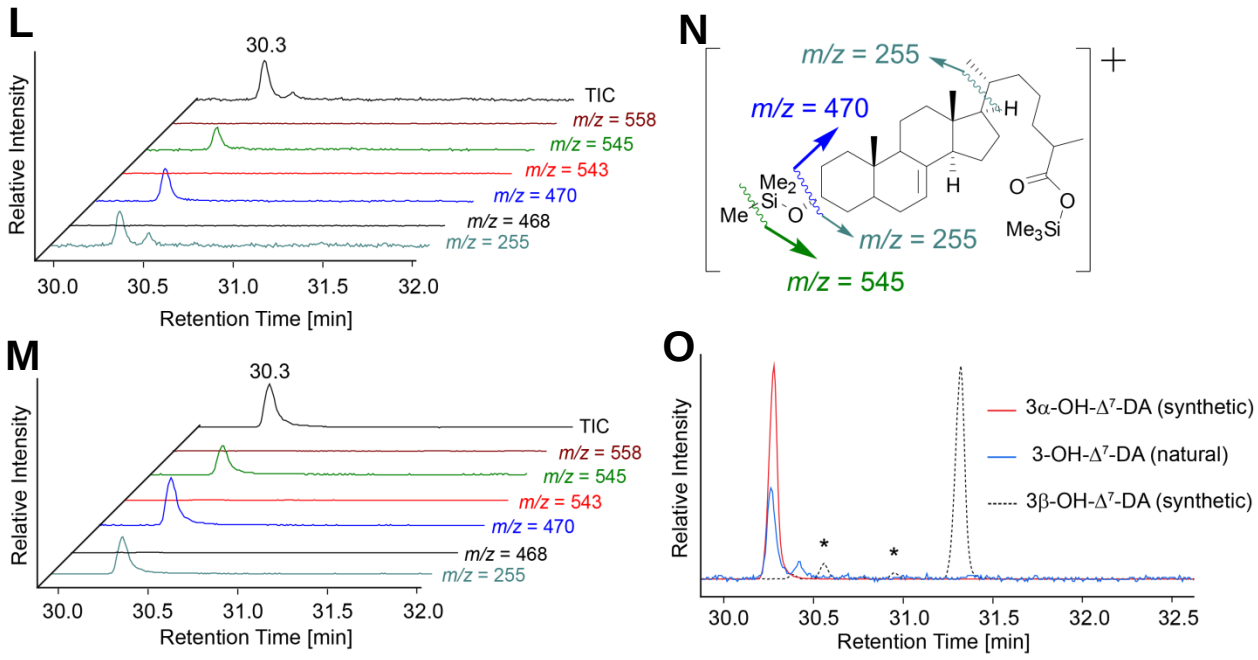

Figure S2, related to Figure 3. Identification of *C. elegans* cholesterol metabolites via DANS and SIM-GC/MS. (L) Ion chromatograms from SIM-GC/MS analysis of a silylated sample of active HPLC-fraction derived from *daf-22* active region II, indicating the presence of the trimethylsilyl- (TMS) derivative of 3α-OH-Δ^7-DA. **(M)** Ion chromatograms from SIM-GC/MS analysis of a silylated sample of synthetic 3α-OH-Δ^7-DA. **(N)** EI-MS fragmentation pattern of the trimethylsilyl (TMS) derivative of 3α-OH-Δ^7-DA. **(O)** GC/MS total ion chromatograms (TIC) from SIM-GC/MS analysis of TMS-derivatized synthetic 3α-OH-Δ^7-DA, synthetic 3β-OH-Δ^7-DA, and *daf-22* mutant metabolome fraction, indicating the presence of 3α-OH-Δ^7-DA in the natural sample. (*) indicates signals derived from small amounts of impurities in the synthetic 3β-OH-Δ^7-DA sample.

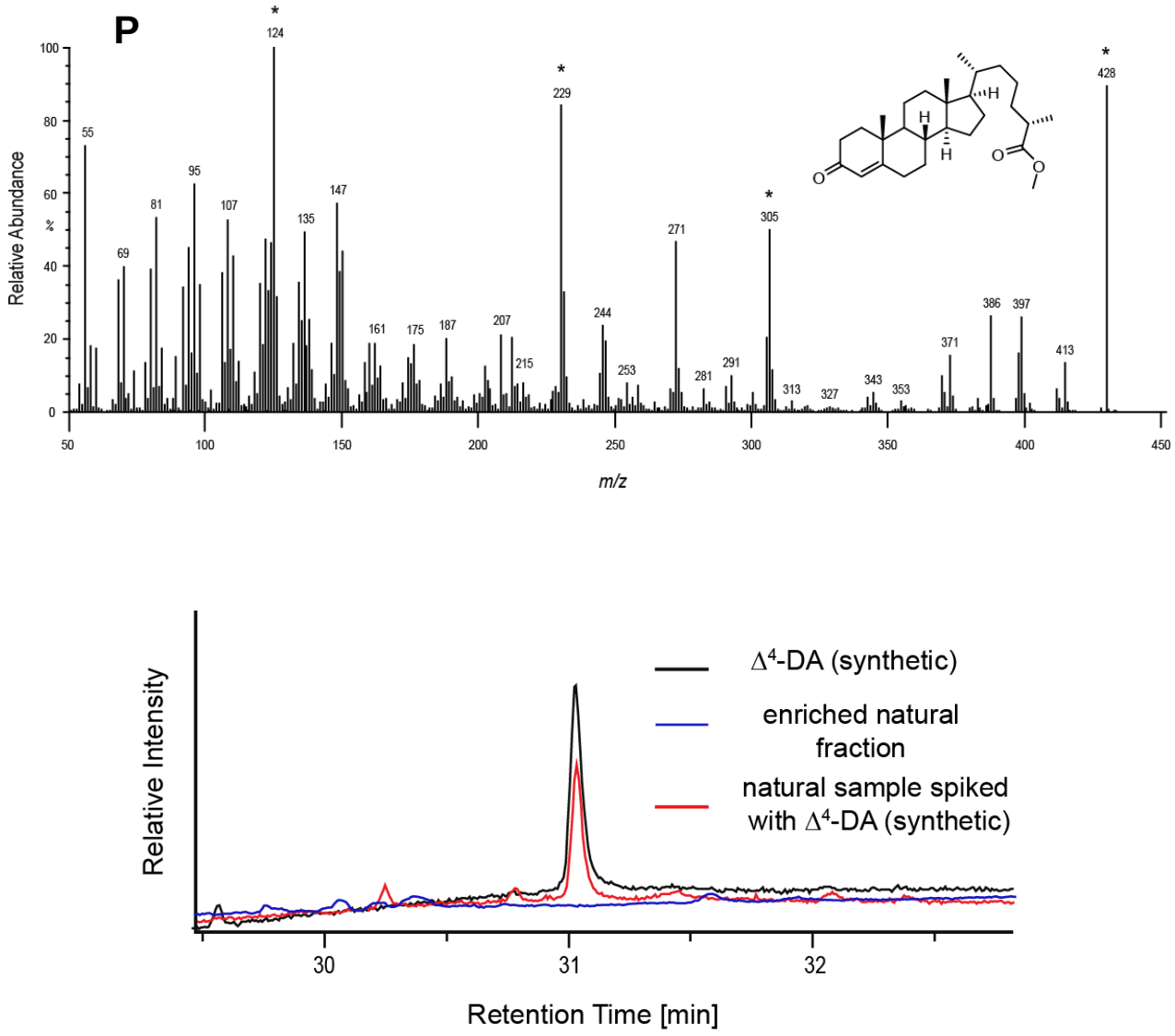

Figure S2, related to Figure 3. Identification of *C. elegans* cholesterol metabolites via DANS and SIM-GC/MS. (P) EI-MS for Δ^4-DA methyl ester (top). (*) Indicates the fragment ions subsequently used for SIM-GC/MS analysis of this compound in natural samples. SIM-GC/MS total ion chromatograms (TIC) of synthetic Δ^4-DA methyl ester, methylated inactive fraction 26 from *daf-22* spiked with synthetic Δ^4-DA (100 ng, ~20-fold less than Δ^7-, $\Delta^{1,7}$-DAs in active metabolome fractions), and methylated *daf-22* metabolome HPLC fraction including the expected elution window of Δ^4-DA (bottom)**.**

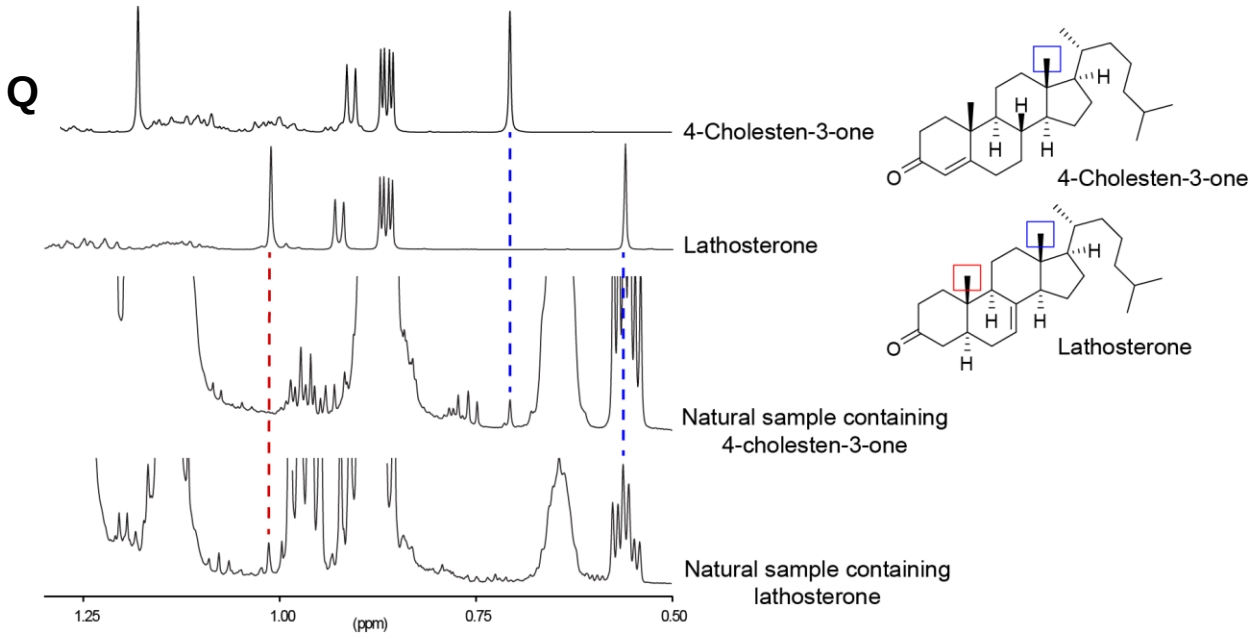

Figure S2, related to Figure 3. Identification of *C. elegans* cholesterol metabolites via DANS and SIM-GC/MS. (Q) Comparison of representative sections of ^{1}H NMR spectra of ligand-enriched *daf-22* metabolome fractions, synthetic 4-cholesten-3-one, and synthetic lathosterone indicating the presence of these two 3-keto-steroids in the natural sample.

R

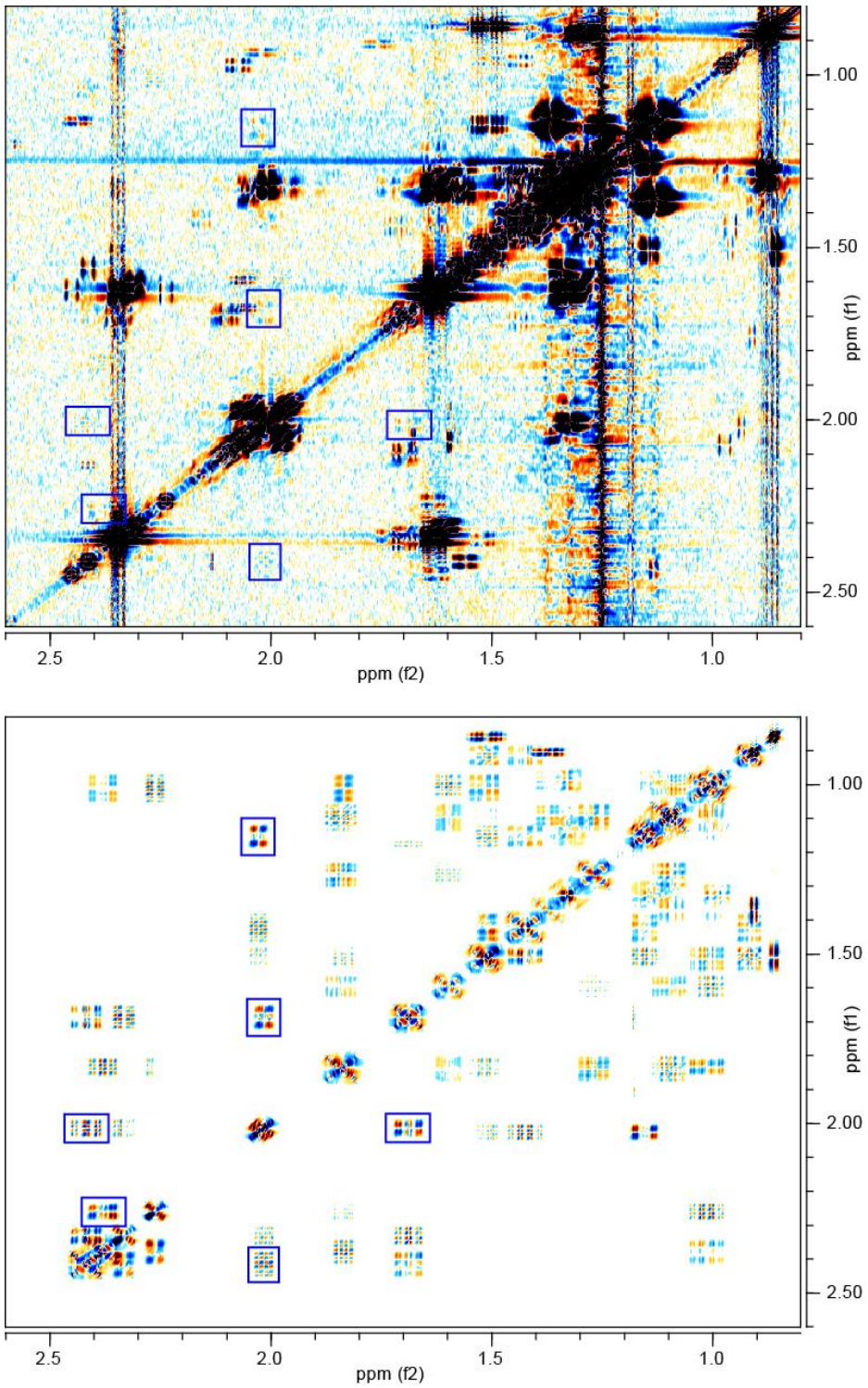

Figure S2, related to Figure 3. Identification of *C. elegans* cholesterol metabolites via DANS and SIM-GC/MS. (R) Section of dqfCOSY spectrum (600 MHz, $CDCl_3$) of *daf-22* metabolome fraction. Signals marked with blue boxes indicate the presence of 4-cholesten-3-one (top). Corresponding section of spectrum of synthetic 4-cholesten-3-one (bottom).

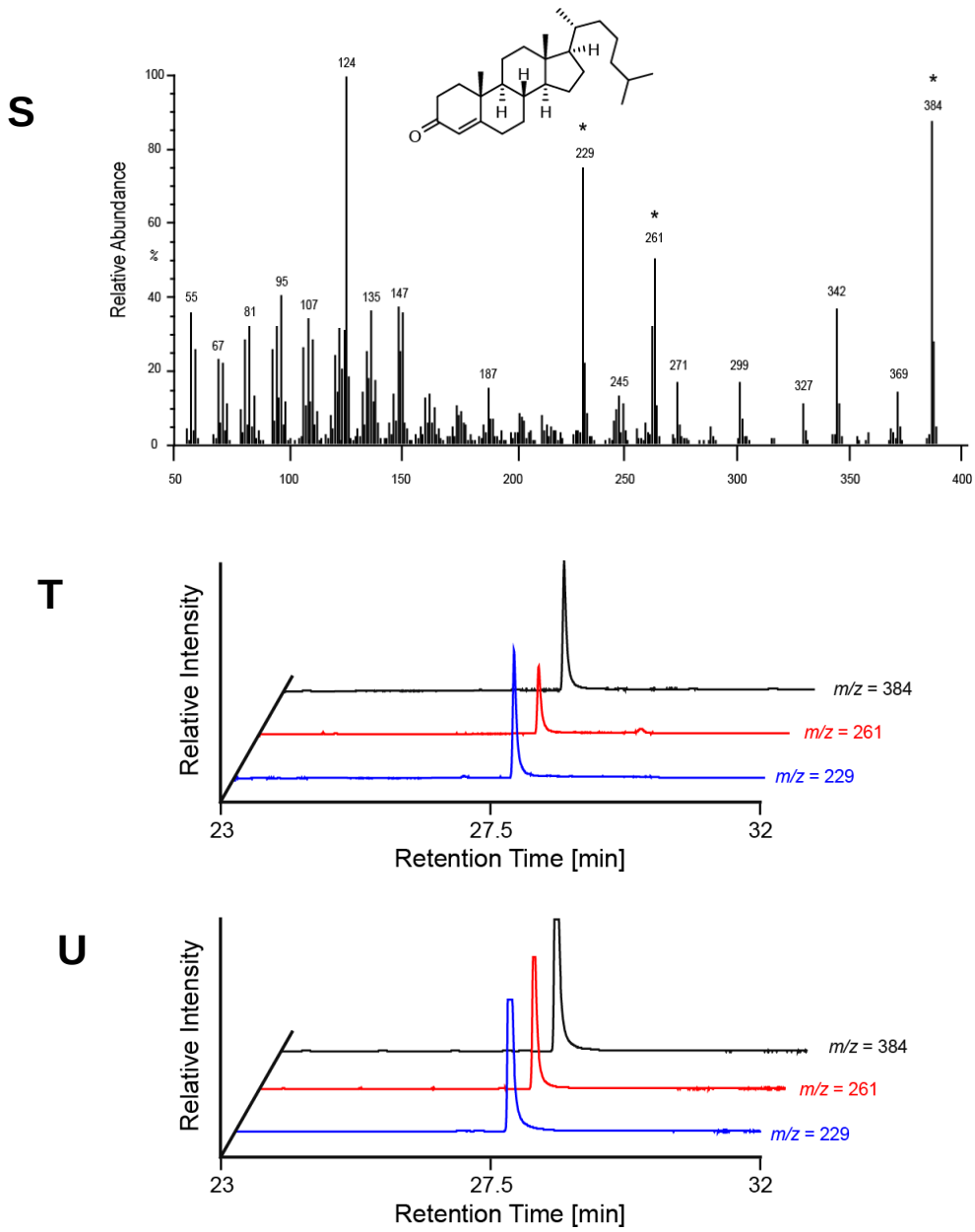

Figure S2, related to Figure 3. Identification of *C. elegans* cholesterol metabolites via DANS and SIM-GC/MS. (S) EI-MS for 4-cholesten-3-one. (*) Indicates the fragment ions subsequently used for SIM-GC/MS-based analysis of this compound in natural samples. **(T)** Ion chromatograms from SIM-GC/MS analysis of *daf-22* mutant metabolome fractions, showing peaks indicative of 4-cholesten-3-one. **(U)** Ion chromatograms from the analysis of a sample of synthetic 4-cholesten-3-one.

V

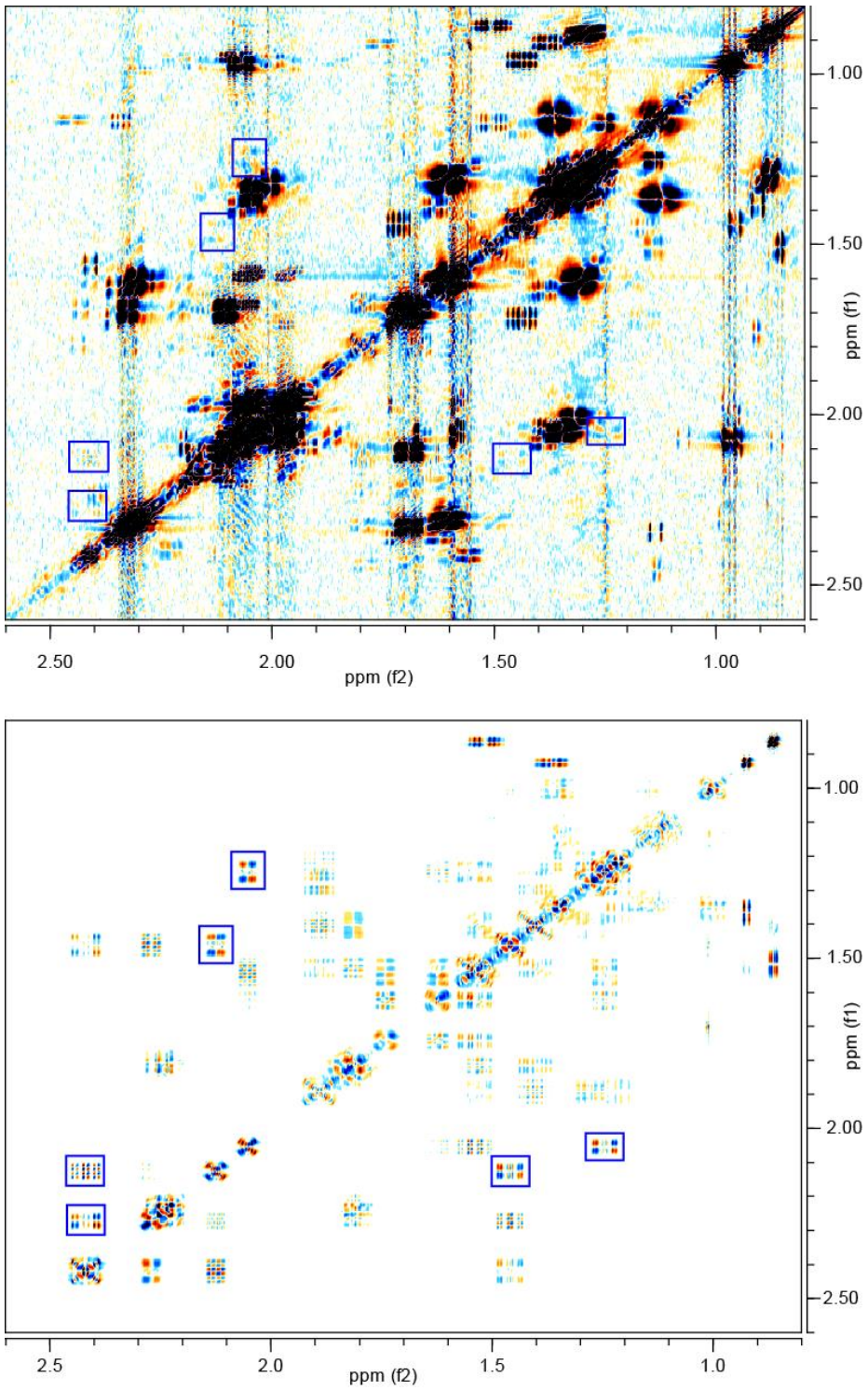

Figure S2, related to Figure 3. Identification of *C. elegans* cholesterol metabolites via DANS and SIM-GC/MS. (V) Section of dqfCOSY spectrum (600 MHz, $CDCl_3$) of *daf-22* metabolome fraction. Signals marked with blue boxes indicate the presence of lathosterone (top). Corresponding section of the spectrum of synthetic lathosterone (bottom).

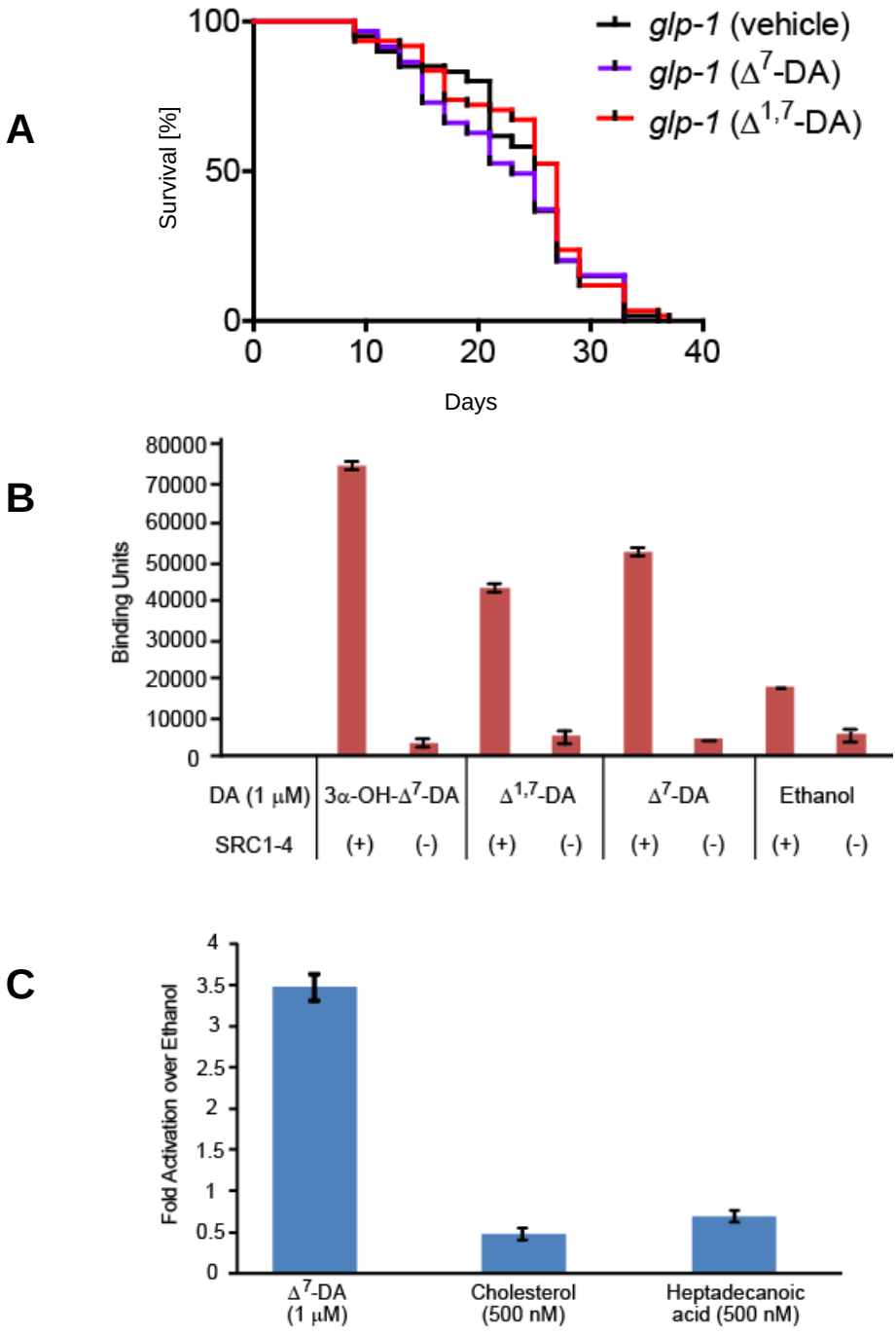

Figure S3. DAF-12 ligand bioactivity and comparative metabolomic analysis of mutant metabolome fractions. (A), related to Figure 5C. Lifespan extension in germline-deficient *glp-1* mutants is not affected by the addition of 100 nM of the most abundant DAF-12 ligand candidates, Δ^7- and $\Delta^{1,7}$-DA. **(B), related to Figure 5D.** DAF-12-ligand candidates produce SRC1-4 dependent signal in the Alphascreen. Shown are data obtained from one day of experiments (N = 4). Figure 4H shows combined data derived from three or more independent experiments (each N = 4 or higher) run on at least three different days (error bars, ±SD). **(C), related to Figure 5D.** Cholesterol and heptadecanoic acid do not produce signal in the Alphascreen assay (error bars, ±SD).

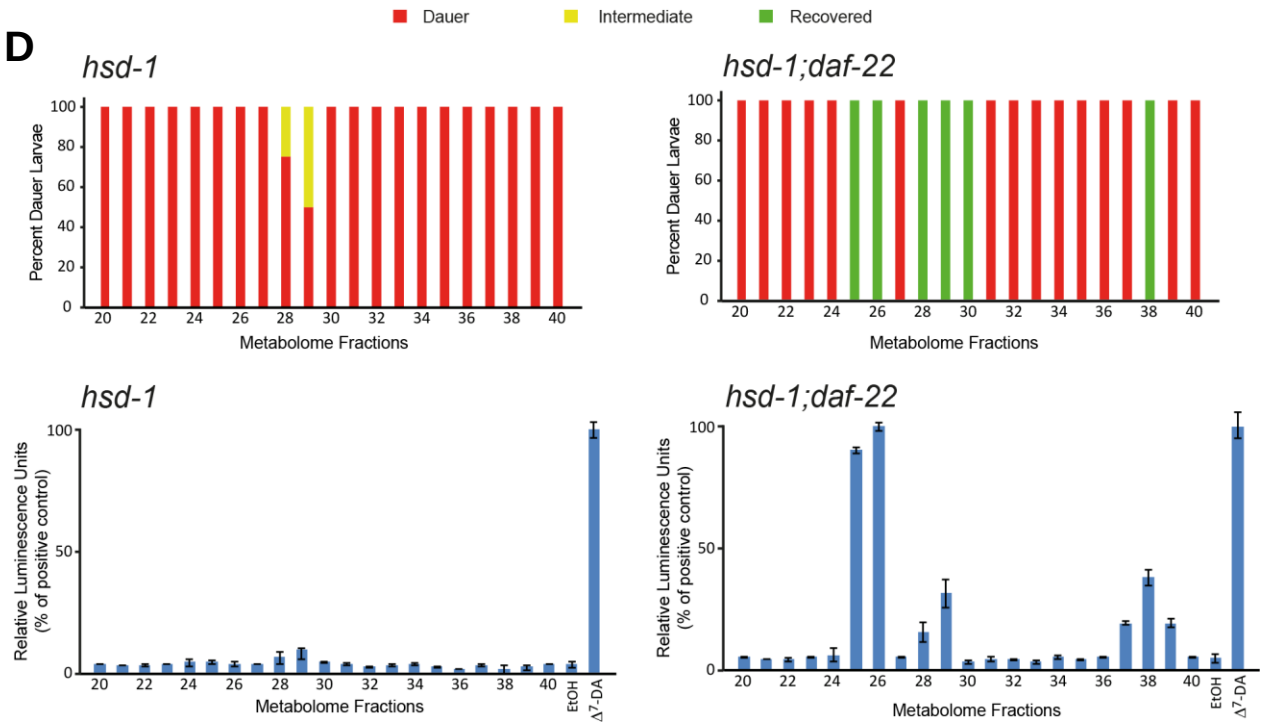

Figure S3, related to Figure 5E. DAF-12 ligand bioactivity and comparative metabolomic analysis of mutant metabolome fractions. (D) Assessment of DAF-12 ligand content using the *in vivo daf-9(dh6)* dauer rescue (top) and the *in vitro* luciferase assay in HEK-293T cells (bottom) with metabolome fractions from *hsd-1* and *hsd-1;daf-22* mutant worms. For the *in vitro* luciferase assay 100 nM Δ^7-DA was used as a positive control (error bars, ±SD).

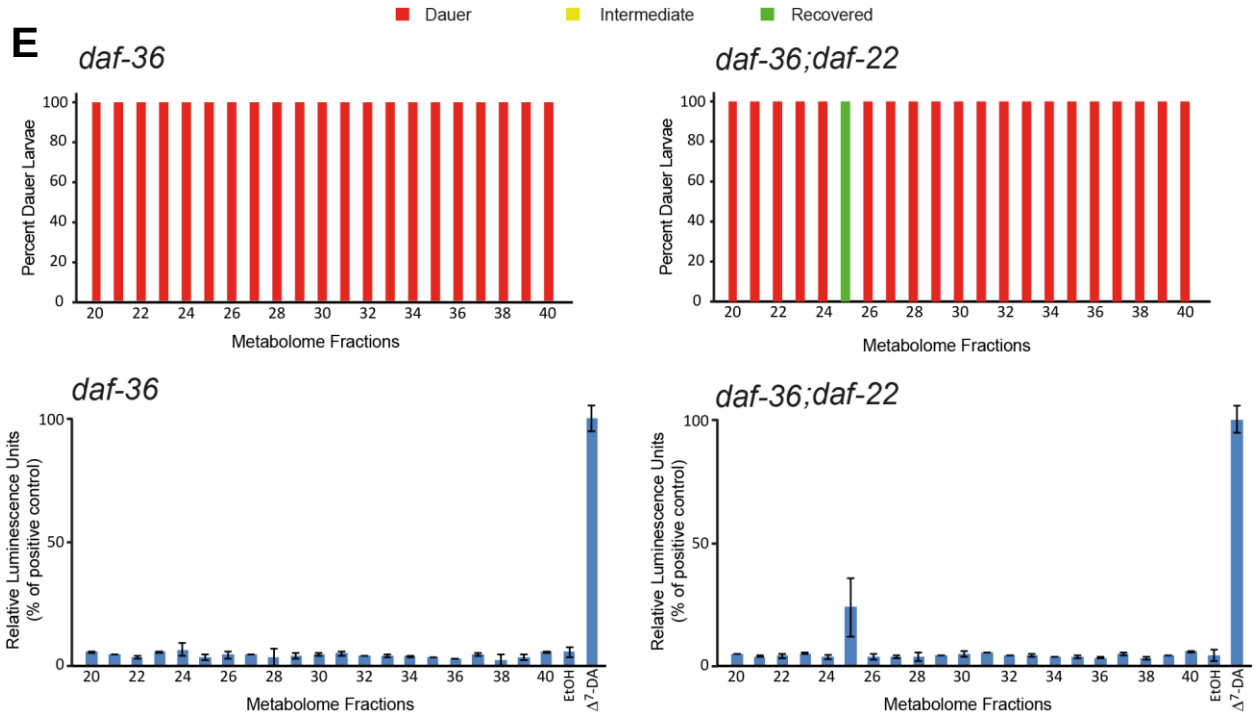

Figure S3, related to Figure 5E. DAF-12 ligand bioactivity and comparative metabolomic analysis of mutant metabolome fractions. (E) Assessment of DAF-12 ligand content using the *in vivo daf-9(dh6)* dauer rescue (top) and the *in vitro* luciferase assay in HEK-293T cells (bottom) with metabolome fractions from *daf-36* and *daf-36;daf-22* mutant worms. For the *in vitro* luciferase assay 100 nM Δ^7-DA was used as a positive control (error bars, ±SD).

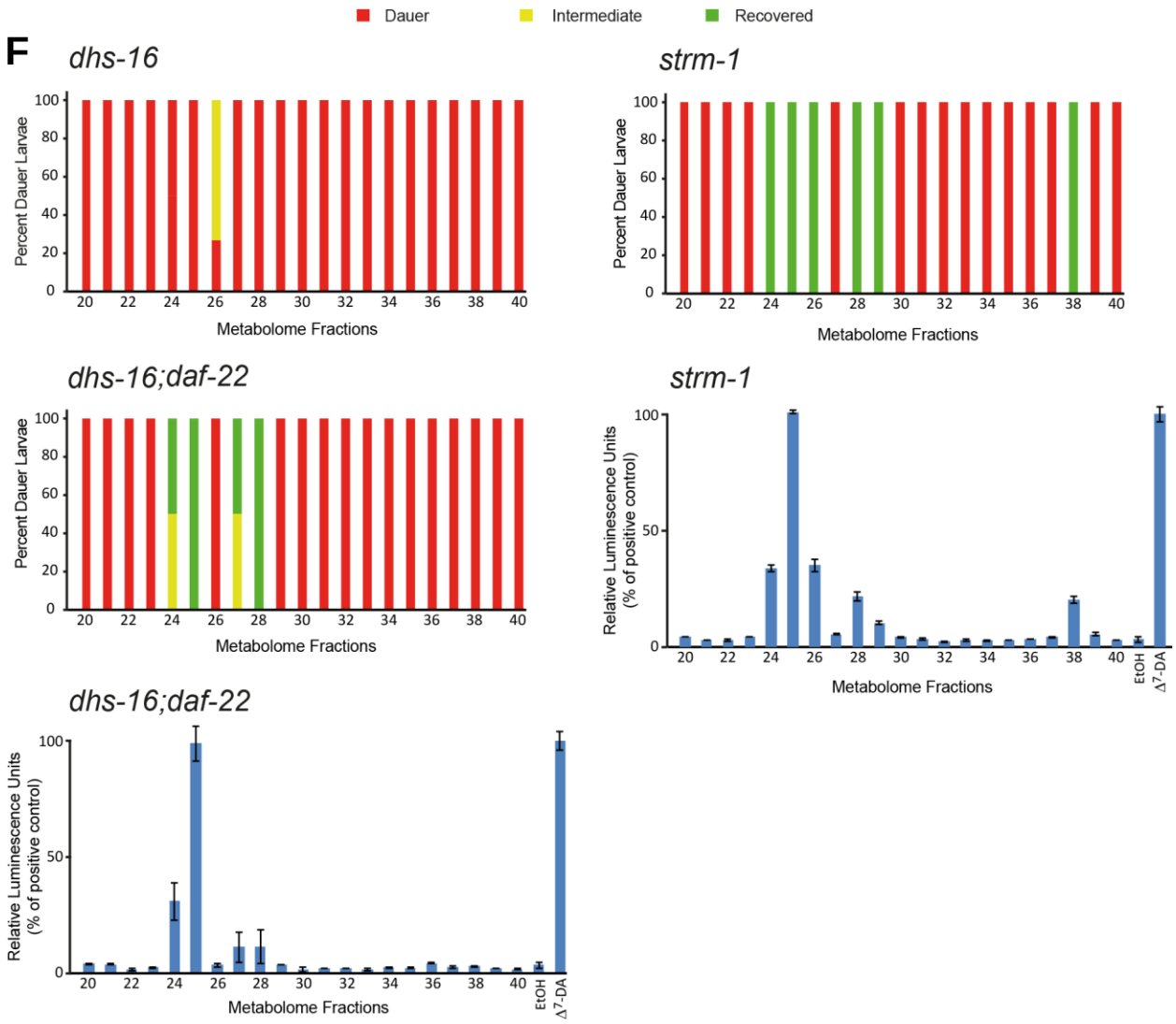

Figure S3, related to Figure 5E. DAF-12 ligand bioactivity and comparative metabolomic analysis of mutant metabolome fractions. (F) Assessment of DAF-12 ligand content using the *in vivo daf-9(dh6)* dauer rescue and the *in vitro* luciferase assay in HEK-293T cells with metabolome fractions from *dhs-16*, *dhs-16;daf-22*, and *strm-1*. The less sensitive *in vitro* luciferase assay was not conducted for *dhs-16* metabolome fractions. 100 nM Δ^7-DA was used as a positive control for the *in vitro* luciferase assay (error bars, ±SD).

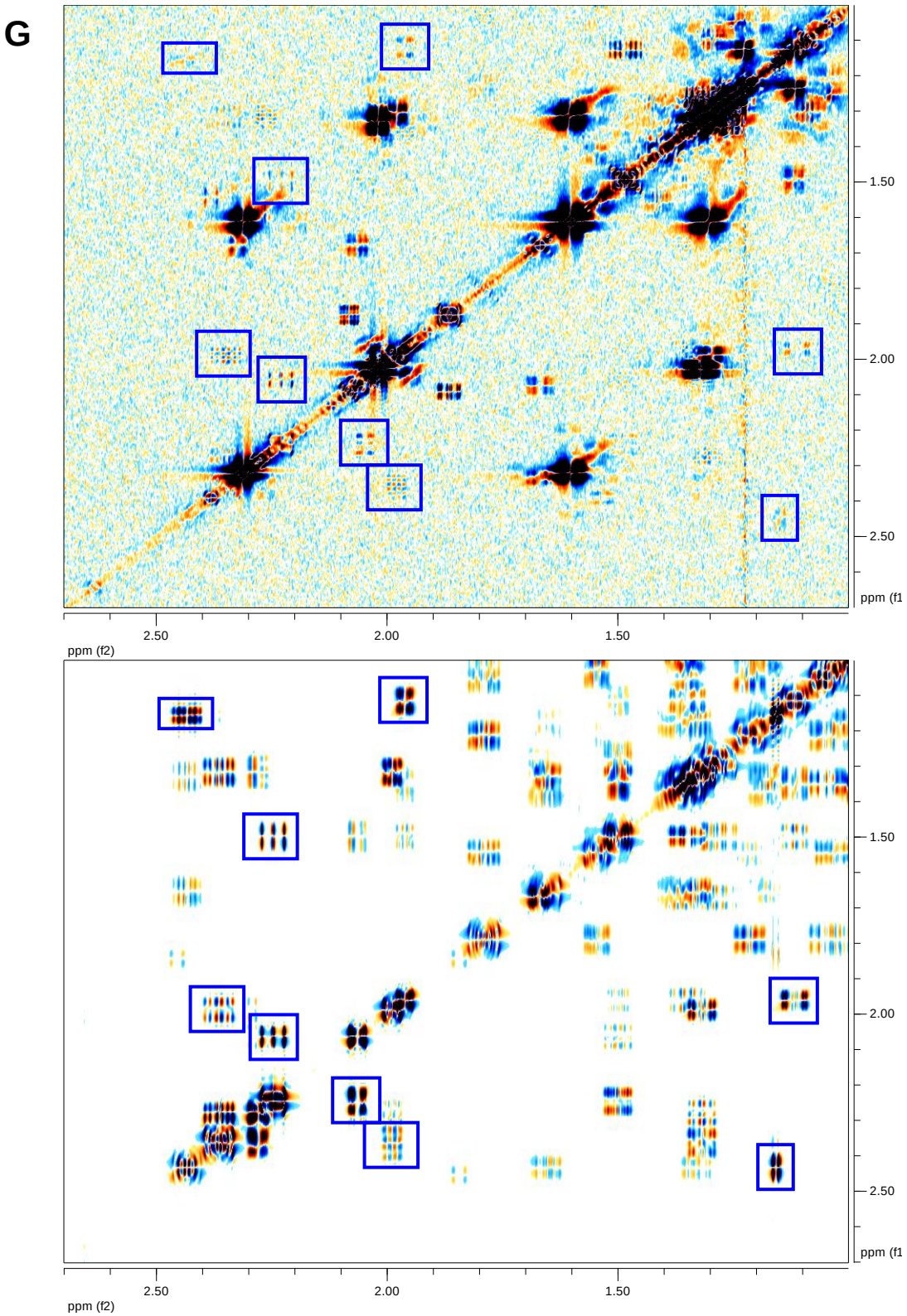

Figure S3, related to Figure 5E. DAF-12 ligand bioactivity and comparative metabolomic analysis of mutant metabolome fractions. (G) Section of dqfCOSY spectrum (600 MHz, $CDCl_3$) of HPLC fraction from the *hsd-1;daf-22* mutant metabolome (top). Crosspeaks indicative of Δ^0-DA are boxed blue. Corresponding section of the spectrum of synthetic Δ^0-DA (bottom).

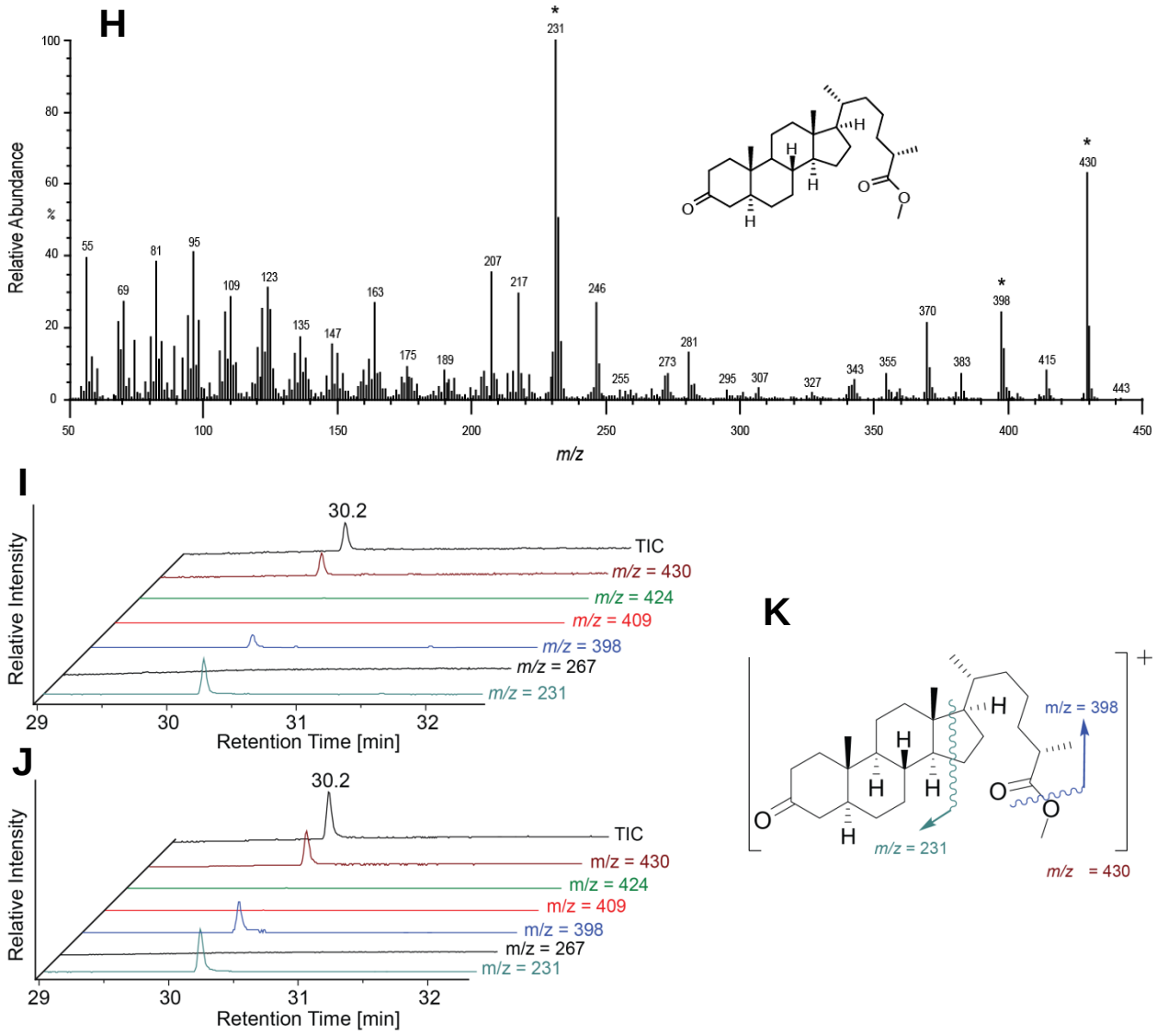

Figure S3, related to Figure 5E. DAF-12 ligand bioactivity and comparative metabolomic analysis of mutant metabolome fractions. (H) EI-MS spectrum of Δ^0-DA methyl ester. (*) Indicates the fragment ions subsequently used for SIM-GC/MS analysis of Δ^0-DA in natural samples. **(I)** SIM-GC/MS analysis of methylated *hsd-1;daf-22* mutant metabolome fraction. Peaks in the shown ion chromatograms are indicative for the presence of Δ^0-DA methyl ester. **(J)** Corresponding ion chormtograms obtained for a sample of methylated synthetic Δ^0-DA. **(K)** EI-MS fragmentation of Δ^0-DA methyl ester used for the SIM-GC/MS analyses in Figures S3J and S3K.

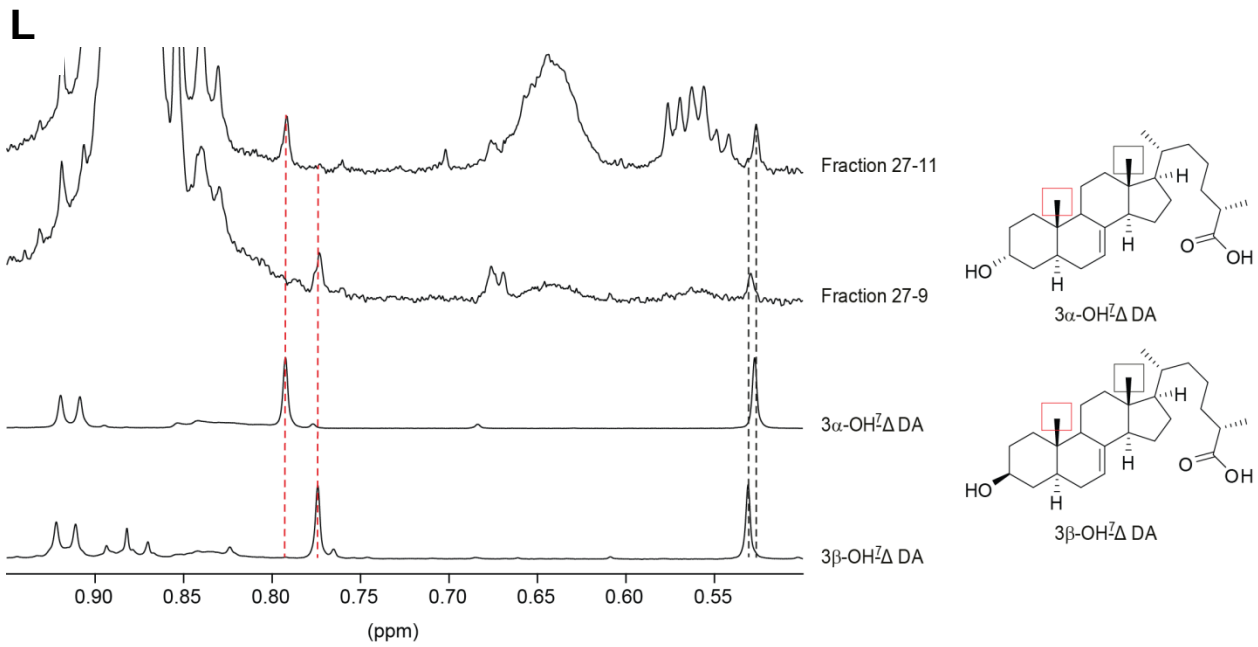

Figure S3, related to Figure 5E. DAF-12 ligand bioactivity and comparative metabolomic analysis of mutant metabolome fractions. (L) Comparison of representative sections of ^{1}H NMR spectra of active HPLC fraction derived from *hsd-1;daf-22* active region II, synthetic 3α-OH-Δ^{7}-DA, and 3β-OH-Δ^{7}-DA. The comparison reveals the presence of 3α-OH-Δ^{7}-DA in fraction 27-11 and 3β-OH-Δ^{7}-DA in fraction 27-9.

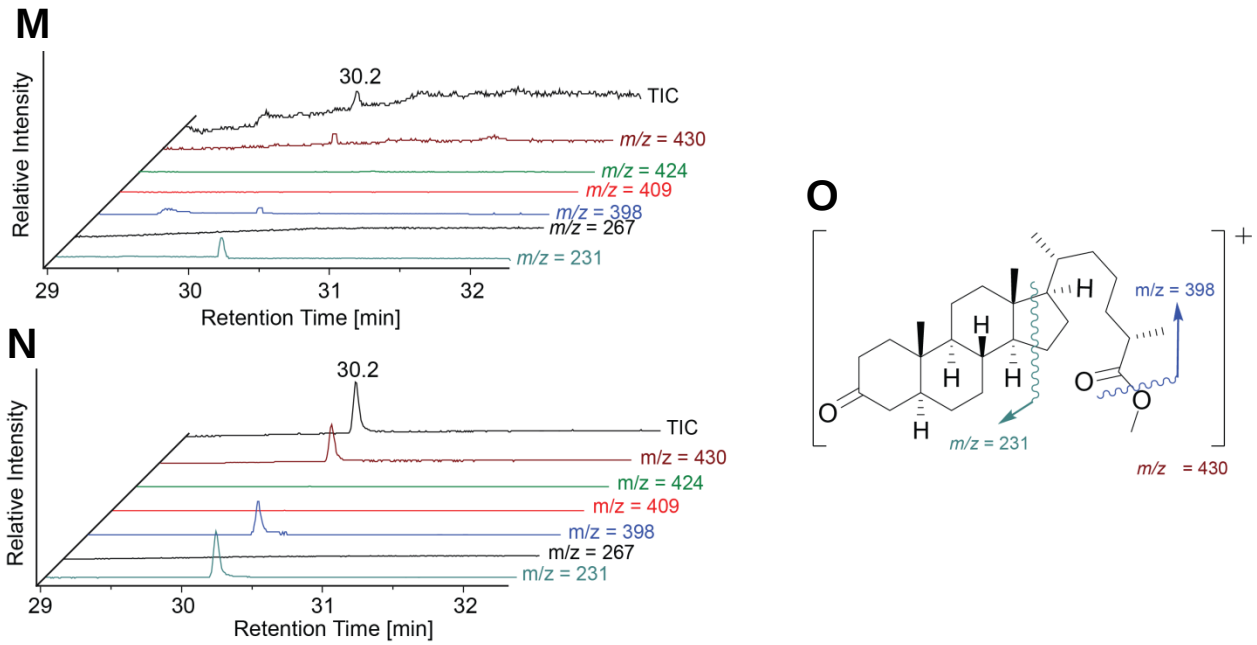

Figure S3, related to Figure 5E. DAF-12 ligand bioactivity and comparative metabolomic analysis of mutant metabolome fractions. (M) Ion chromatograms from SIM-GC/MS analysis of methylated fraction 25 from the *daf-36;daf-22* mutant metabolome, showing peaks indicative of the presence of Δ^0-DA. **(N)** Ion chromatograms from the analysis of a sample of methylated synthetic Δ^0-DA. **(O)** EI-MS fragmentation pattern of Δ^0-DA methyl ester.

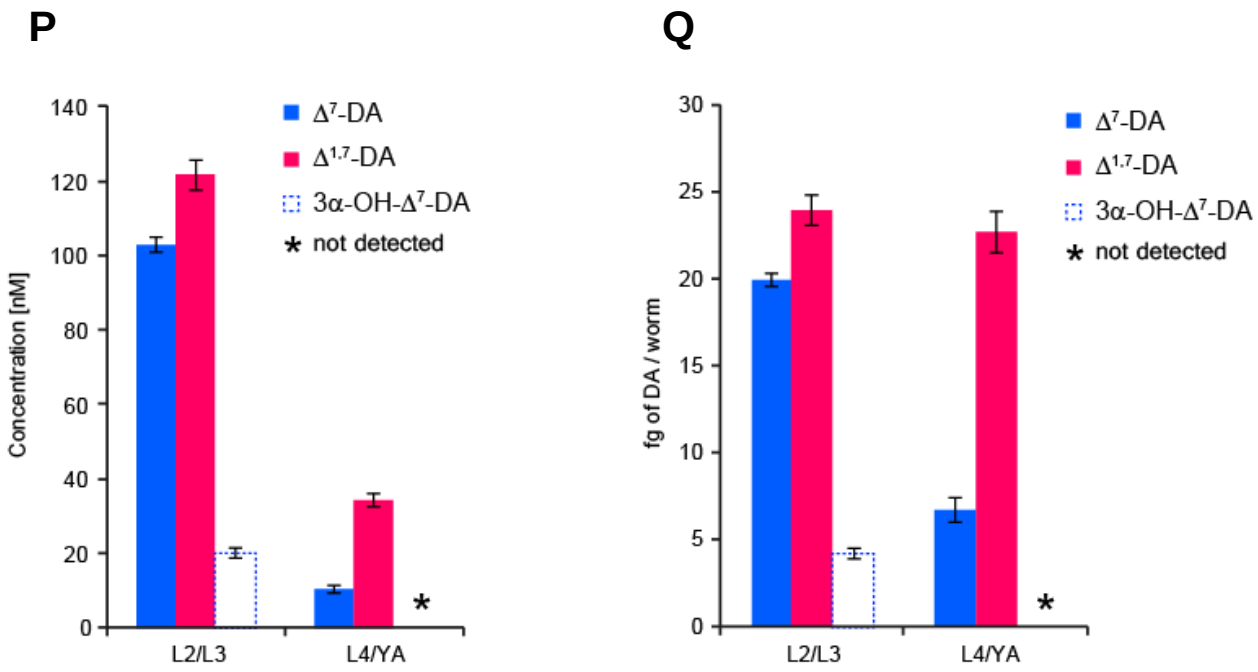

Figure S3, related to Figure 5E. DAF-12 ligand bioactivity and comparative metabolomic analysis of mutant metabolome fractions. (P) *In vivo* concentrations of Δ^7-DA, $\Delta^{1,7}$-DA, and 3α-OH- Δ^7-DA in synchronized wild-type (N2) worms at L2/L3 and L4/young adult (YA) stages, derived from SIM-GC/MS-based quantification (error bars, ±SD). **(Q)** Absolute SIM-GC/MS-based quantification of Δ^7-DA, $\Delta^{1,7}$-DA, and 3α-OH-Δ^7-DA in synchronized wild-type (N2) worms at the L2/L3 and L4/young adult (YA) stages (error bars, ±SD).

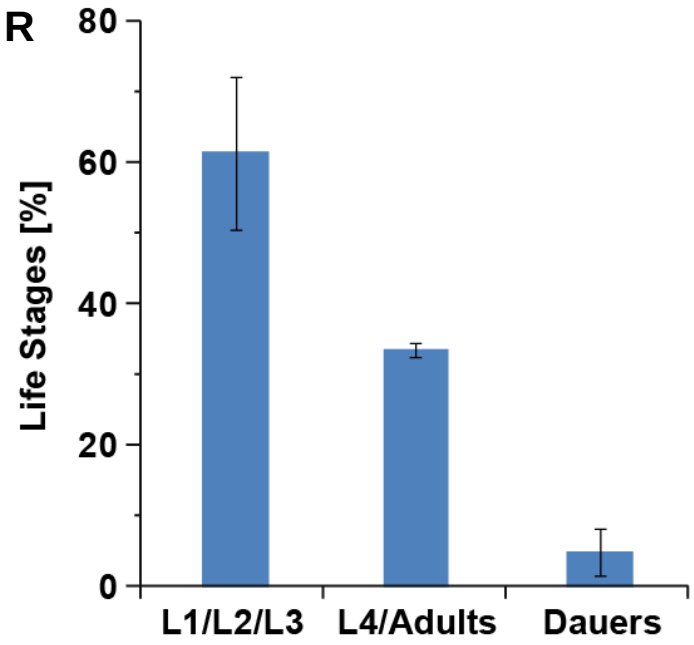

Figure S3, related to Figure 5E. DAF-12 ligand bioactivity and comparative metabolomic analysis of mutant metabolome fractions. (R) Distribution of different stages of *C. elegans* in mixed stage liquid cultures of *daf-22* mutant worms. Calculations are based on analysis of 10 µL liquid culture samples (N = 3) taken from six different 100 mL cultures at harvest time (error bars, ±SD).

SUPPLEMENTAL TABLES

Table S1, related to Figure 3. NMR spectroscopic data of $\Delta^{1,7}$-DA. ^{1}H (600 MHz), ^{13}C (151 MHz), and important HMBC NMR spectroscopic data for $\Delta^{1,7}$-DA in $CDCl_3$. Chemical shifts were referenced to ($C\underline{H}Cl_3$) = 7.26 ppm and ($\underline{C}DCl_3$) = 77.16 ppm.

Carbon No.	δ (ppm)	Proton No.	δ (ppm)	*J* (Hz)	HMBC Correlations
1	157.3	1-H	7.01	$J_{1,2}$=10	C-10, C-9, C-5, C-3
2	127.1	2-H	5.89		C-10, C-4
3	199.8	----	----	----	----
4	40.1	4-H_α	2.34		C-3, C-10
		4-H_β	2.34		C-3, C-10
5	39.6	5-H	2.05		
6	28.7	6-H_α	1.89-1.94		C-8
		6-H_β	1.89-1.94		
7	117.8	7-H	5.25		
8	138.8	----	----	----	----
9	45.2	9-H	1.93		
10	39.6	----	----	----	----
11	21.5	11-H_α	1.76		
		11-H_β	1.58		
12	39.2	12-H_α	1.27		
		12-H_β	2.09		
13	43.5	----	----	----	----
14	55.1	14-H	1.83		
15	23.0	15-H_α	1.53		
		15-H_β	1.42		
16	27.8	16-H_α	1.89		
		16-H_β	1.28		
17	55.9	17-H	1.82		
18	11.9	18-H	0.57	----	C-12, C-13, C-14, C-17
19	12.6	19-H	0.95	----	C-1, C-10, C-5, C-9
20	36.1	20-H	1.38		
21	18.7	21-H	0.93	$J_{21,22}$=6.4	
22	35.7	22-H_α	1.05		
		22-H_β	1.39		
23	23.9	23-H_α	1.21		
		23-H_β	1.39		
24	34.0	24-H_α	1.37		
		24-H_β	1.68		
25	38.9	25-H	2.48	$J_{25,26}$=6.9	C-23, C-24, C-27
26	17.0	26-H	1.19		C-25, C-27, C-24
27	179.3	----	----	----	----

Table S2, related to Figure 3. NMR spectroscopic data of 3α-OH-Δ^7-DA. ^{1}H (600 MHz), ^{13}C (151 MHz), and important HMBC NMR spectroscopic data for 3α-OH-Δ^7-DA in $CDCl_3$. Chemical shifts were referenced to ($C\underline{H}Cl_3$) = 7.26 ppm and ($\underline{C}DCl_3$) = 77.16 ppm.

Carbon No.	δ (ppm)	Proton No.	δ (ppm)	*J* (Hz)	HMBC Correlations
1	31.9	1-H_α	1.43		C-3
		1-H_β	1.55		C-3, C-5
2	28.7	2-H_α	1.4-1.63		
		2-H_β	1.4-1.63		
3	66.4	3-H	4.07	$J_{3\text{-}2}$= 8.7, $J_{3\text{-}4}$= 3.5	
4	35.4	4-H_α	1.40-1.52		
		4-H_β	1.40-1.52		
5	34.6	5-H	1.74	----	C-10
6	29.5	6-H_α	1.67-1.72		
		6-H_β	1.67-1.72		
7	117.5	7-H	5.17		
8	139.6	----	----	----	----
9	49.4	9-H	1.75		
10	34.7	----	----	----	----
11	21.2	11-H_α	1.58		
		11-H_β	1.43		
12	39.5	12-H_α	1.24		
		12-H_β	2.02		
13	43.4	----	----	----	----
14	55.0	14-H	1.80		
15	22.9	15-H_α	1.53		C-8
		15-H_β	1.39		
16	29.6	16-H_α	1.86		
		16-H_β	1.25		
17	55.9	17-H	1.20		
18	11.9	18-H	0.53		C-12, C-13, C-14, C17
19	12.0	19-H	0.77		C-1, C-10, C-5, C-9
20	36.0	20-H	1.36		
21	18.9	21-H	0.92	$J_{21\text{-}20}$ = 6.5	C-20, C-17, C-22
22	35.7	22-H_α	1.38		
		22-H_β	1.05		
23	23.7	23-H_α	1.20		
		23-H_β	1.36		
24	34.0	24-H_α	1.37		
		24-H_β	1.66		
25	38.8	25-H	2.49	$J_{25\text{-}26}$ = 7.0	C-23, C-24, C-27
26	17.0	26-H	1.19		C-24, C-25, C-27
27	179.0	----	----	----	----

Table S3, related to Figure 5. Bioactivity of synthetic DAs. EC_{50} values of synthetic DAs in luciferase, Alphascreen, and *daf-9(dh6)* dauer rescue assays and the HPLC retention times of synthetic DAs.

Compound	EC_{50} (nM) for luciferase assay (*in vitro*)	EC_{50} (nM) for Alphascreen assay (*in vitro*)	EC_{50} (nM) for *daf-9(dh6)* dauer rescue assay (*in vivo*)	HPLC retention time ranges (mins)
$\Delta^{1,7}$-DA	146	15	2	20.5-20.9
Δ^{7}-DA	39	8	3	20.9-21.5
Δ^{0}-DA	411	not determined	19	24-25
3α-OH-Δ^{7}-DA	240	200	6	21-22
3β-OH-Δ^{7}-DA	not determined	not determined	22	18-19

SUPPLEMENTAL EXPERIMENTAL PROCEDURES

Protocols Used for the Large-scale Fractionation of Worm Pellet Extract

To 8 g of Celite, prewashed with ethyl acetate, was added a solution of worm pellet metabolome extract from 16 cultures. After evaporation of the solvent, the Celite® was dry-loaded into an empty 25 g RediSep *Rf* loading cartridge. Fractionation was performed using a Teledyne ISCO CombiFlash system over a RediSep*Rf* GOLD 40 g HP Silica Column using a normal phase dichloromethane-methanol solvent system, starting with 6 min of 100% dichloromethane, followed by a linear increase of methanol content up to 10% at 24 min, followed by another linear increase of methanol content up to 40% at 40 min, followed by another linear increase of methanol content up to 95% at 45 min which was then continued to 48 min. 70 fractions (~20 mL each) generated from the combiflash run were individually evaporated *in vacuo* and prepared for bio-assays and analyses by NMR spectroscopy (^{1}H NMR, dqfCOSY), HPLC-MS, and GC/MS.

For the quantification of lathosterone and 4-cholesten-3-one in *daf-22(m130)* worms, fractions 4-10 from the set of 70 fractions were combined and added to 4 g of Celite that had been prewashed with ethyl acetate. After evaporation of the solvent, the Celite was dry-loaded into an empty 12 g RediSep *Rf* loading cartridge. Fractionation was performed using the CombiFlash system and a RediSep *Rf* GOLD 24 g HP silica column using a hexanes-ethyl acetate solvent system, starting with 4.8 min of 100% hexanes, followed by a linear increase of ethyl acetate content up to 40% at 43.2 min to generate 130 fractions (~12 mL each). A synthetic mixture of lathosterone and 4-cholesten-3-one was subsequently run following an identifcal CombiFlash protocol. A range of fractions from the natural sample run that corresponded to the elution profiles of the synthetic 3-keto steroids were individually evaporated *in vacuo* and analyzed by NMR spectroscopy (^{1}H NMR, dqfCOSY) and GC/MS for quantification of lathosterone and 4-cholesten-3-one.

For the fractionation of metabolomes derived from staged L2/L3 and L4/YA worm pellets, the metabolome extracts were added to 2 g of Celite (prewashed with ethyl acetate). After evaporation of the solvent, the Celite was dry-loaded into an empty 5 g RediSep *Rf* loading cartridge. Fractionation was performed using a Teledyne ISCO CombiFlash system and a RediSep*Rf* GOLD 4 g HP Silica Column using a dichloromethane-methanol solvent system, starting with 1.25 min of 100% dichloromethane, followed by a linear increase of methanol

content up to 10% at 3.2 min, followed by another linear increase of methanol content up to 40% at 9 min, followed by another linear increase of methanol content up to 95% at 10.2 min which was then continued to 10.7 min. 70 fractions (~3 mL each) generated in this manner were individually evaporated *in vacuo* and prepared for dauer rescue assays using *daf-9(dh6)* worms and subsequent analysis by SIM-GC/MS.

Protocol for further Fractionation via HPLC

Metabolome fractions of interest were evaporated *in vacuo*, resuspended in 250 μL of methanol and submitted to HPLC analysis, using an Agilent 1100 Series HPLC system equipped with an Agilent Eclipse XDB C-18 column (25 cm x 9.4 mm, 5 μm particle diameter). A 0.1% acetic acid in water ("aqueous") – 9:1 acetonitrile:methanol ("organic") solvent system was used, starting with 70% organic solvent for 3 min, which was increased linearly to 100% over a period of 20 min and continued at 100% organic solvent for 2 min. One-minute fractions were collected using a Teledyne ISCO Foxy 200 X-Y fraction collector from 12 to 36 min. Collected fractions were individually evaporated *in vacuo* for further analysis by GC-MS or NMR spectroscopy.

***daf-9(dh6)* Dauer Rescue Assay (Liquid Culture Assay)**

Individual metabolome fractions were dried *in vacuo* and resuspended in 500 μL EtOH. 20-25 gravid *daf-9(dh6)* adults were picked onto three 6 cm NGM agar plates seeded with OP50 containing 25 μL of 10 μM Δ^7-DA each and allowed to grow for three days. On the third day each of the plates was washed with M9 and treated with alkaline hypochlorite solution to obtain eggs. Isolated eggs were allowed to hatch overnight in S-complete media without food. 100 μl of the resulting synchronized L1 suspension was added to 400 μL of HB101-seeded S-complete media and 5 μL of ethanol, ethanol suspension of metabolome fractions, or ethanol solution of synthetic ligands (1.25 nM – 200 nM) per well of a 12 well plate. Wells were examined after 48 and 72 h and scored for dauers, recovered animals, and intermediate worms with molting defects and/or Mig phenotypes. For active metabolome fractions, additional assays using smaller amounts were conducted.

For dauer assays with metabolome fractions from staged L2/L3 and L4/young adult cultures, the above protocol was modified as follows. The metabolome fractions were resuspended in 20 μL EtOH. 20-25 gravid *daf-9(dh6)* adults were picked onto three 6 cm NGM agar plates seeded with OP50 containing 25 μL of 10 μM Δ^7-DA each and allowed to grow for three days. On the third

day each of the plates was washed with M9 and treated with alkaline hypochlorite solution to obtain eggs. Isolated eggs were allowed to hatch overnight in S-complete media without food. 10 µl of the resulting synchronized L1 suspension was added to 40 µL of HB101-seeded S-complete media and 0.5 µL of ethanol, ethanol suspension of metabolome fractions, or ethanol solution of synthetic ligands (10 nM of Δ^7-DA as positive control) per well of a 96 well plate. Wells were examined after 48 and 72 h and scored for dauers, recovered animals and intermediate worms with molting defects and/or Mig phenotypes.

Alphascreen Assay (DAF-12 direct binding assay)

The Alphascreen assay was used to measure ligand dependent interaction between a heterologously expressed DAF-12 construct and the mammalian co-activator peptide, SRC1-4. An N-terminally GST-6xHis-tagged DAF-12 construct (amino acids 281-753, which includes most of the hinge region and the entire ligand binding domain, LBD) was purified from BL21 (DE3) cells (Sigma) using a GT sepharose column followed by a size exclusion column. Purified DAF-12 (25 nM final concentration) and biotinylated SRC1-4 (synthetic biotin-QKPTSGPQTPQAQQKSLLQQLLTE obtained from Anaspec, used at 50 nM final concentration), were incubated separately in plastic tubes for 20 min with Ni^{2+} chelate acceptor beads (for DAF-12) or streptavidin donor beads (for SRC1-4, 25 µg/mL final concentration, Perkin Elmer, Cat. No - 6760619C). They were then combined with subsequent addition of ligand candidates or ethanol (stored in glass vials) to obtain a final volume of 20 µL, and incubated for 60 min in white, low volume, 384 well Optiplates (Perkin Elmer). The plates were then read using a Synergy 2 Biotek LC luminometer using the manufacturer's Alphascreen detection protocol. All solutions were made using assay buffer containing 25 mM HEPES (pH 7.4) and 100 mM NaCl. Cholesterol and heptadecanoic acid, assayed at 1 µM concentration as additional negative controls, gave no signal (Figure S3C). Addition of CHAPS (40 µM) did not significantly affect assay results, whereas addition of 0.01% BSA reduced signal. All incubations were carried out at room temperature in the dark. Figure 5D shows combined data derived from independent experiments (each N = 4 or higher) run on at least three or more different days.

Life Span Assays

Life span assays were performed in Percival I-36NL incubators at 20 °C. After alkaline hypochlorite treatment and two generations of growth, animals were raised at 25 °C, and sterile

young adult animals were placed onto NGM plates seeded with 10X concentrated *E. coli* OP50, containing 100 nM $\Delta^{1,7}$-DA, Δ^{7}-DA, or ethanol vehicle control. Every fourth day, animals were transferred to new NGM plates with freshly added $\Delta^{1,7}$-DA, Δ^{7}-DA, or vehicle control. Activity of $\Delta^{1,7}$-DA or Δ^{7}-DA, in each batch of plates was confirmed by assessing the ability of the compounds to rescue *daf-9(dh6)* dauer arrest, compared to vehicle control. Animal viability was assessed visually or with gentle prodding. GraphPad Prism (GraphPad Software, La Jolla, CA) was used for data representation and statistical analysis.

GC/MS Instrumentation and Sample Preparation

GC/MS analysis was carried out with an Agilent Technologies 6890N Network GC system with a DB-5MS+DG column (25 µm, 30 m x 0.25 mm) operating in split-less mode, connected to a JEOL JMS-GCmateII mass spectrometer. Methylation of 3-keto-DAs: synthetic standards or 1-10 % of active metabolome fractions were evaporated *in vacuo* and resuspended in toluene:methanol (500 µL, 3:2), followed by the drop-wise addition of trimethylsilyldiazomethane (120 µL, 2 M solution in Et_2O) with stirring. The reaction was stirred at room temperature for 30 min, quenched with acetic acid, evaporated *in vacuo*, and resuspended in dichloromethane (30-200 µL). Of this solution, 1-5 µL were injected per GC/MS analysis. Silylation of 3-hydroxy-DAs: Synthetic standards or 1-10 % of active fractions were evaporated *in vacuo* and a mixture (100 µL) of 3% 1-(trimethylsilyl)imidazole (TMSIM) in *N*-methyl-*N*-(trimethylsilyl)trifluoroacetamide (MSTFA) was added with stirring at 80 °C for 45 min. The reaction mixture was evaporated *in vacuo* and resuspended in dichloromethane (30-200 µL). Of this solution, 1-5 µL were injected per GC/MS run.

GC/MS Methods

GC conditions: Injector was kept at 240 °C and 1 mL/min helium flow was maintained. Initial column temperature was at 120 °C for 1.4 min, then increased to 320 °C at a rate of 7 °C/min, and maintained at 320 °C for 10 min.

MS conditions: Electron impact ionization (EI) at 70 eV was used. For synthetic samples (high concentrations, >100 ng/µL), MS was first operated in scanning mode for a mass range of *m/z* 35-500 for 3-keto-DA methyl ester and 3-keto-steroids, and *m/z* 35-650 for 3-OH-DA TMS derivatives to select for the most abundant fragment ions for each compound. For low concentrations (<5 ng/µL) of synthetic samples and metabolome fractions, MS was operated in

Selective Ion Monitoring (SIM) mode and the following ions were selectively observed: *m/z* = 428, 271, 229 (Δ^7-DA); 426, 269, 227 ($\Delta^{1,7}$-DA); 430, 398, 231 (Δ^0-DA); 428, 305, 229, 124 (Δ^4-DA); 545, 470, 255 (3α- and 3β-OH-Δ^7-DA); 384, 261, 229 (4-cholesten-3-one).

Quantification of DAs from Metabolome Fractions via SIM-GC/MS

GC/MS Data was analyzed using Shrader Analytical and Consulting Laboratories, Inc.'s TSSPro 3.0 software package. Quantification of DAs was performed by integration of GC/MS peaks from the following ion traces: *m/z* = 428 (Δ^7-DA); 426 ($\Delta^{1,7}$-DA); 231 (Δ^0-DA); 428 (Δ^4-DA); 545 (3α- and 3β-OH-Δ^7-DA). Dafachronic acid concentrations were calculated using response factors determined from synthetic standards. Mass spectrometer response was roughly linear (<5% error) for amounts of 10 pg to 5 ng per compound injection.

Statistical Analyses

All data in the supplemental figures are presented as mean ±SD.

Chemical Syntheses and NMR Spectra

(25*S*)-Δ^7-Dafachronic Acid

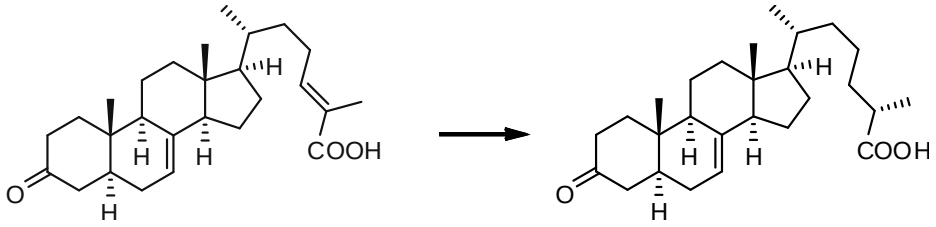

(*E*)-3-keto-5α-cholest-7,24-enoic acid **(25*S*)-Δ^7-DA**

A dry 100 mL Schlenk flask was charged with (*E*)-3-keto-5α-cholest-7,24-enoic acid (62 mg, 0.15 mmol, 1.0 equiv.) (Judkins, J.C., et al. *Angew. Chem.*, in revision), Teflon®-coated magnetic stir bar, and methanol (10 mL). The flask was equipped with a reflux condenser and, while stirring, was flushed with argon for 15 minutes. *(S)*-Ru(OAc)$_2$[H_8-BINAP] (5 mg, 6 μmol, 0.04 equiv.) dissolved in methanol (5 mL) was then added. The reaction flask was warmed to 50 °C and flushed with a vigorous flow of hydrogen for one minute. The hydrogen flow rate was decreased to a slow and steady rate and the reaction was allowed to stir for three hours. The reaction was concentrated *in vacuo* and flash column chromatography on silica gel using a 0-60% (*v/v*) gradient of ethyl acetate containing 0.25% acetic acid in hexanes afforded (25*S*)-Δ^7-dafachronic acid (60 mg, 0.14 mmol, 97%) as a white crystalline solid. NMR and optical rotation data matched those reported previously (Giroux and Corey, 2007).

(25*R*)-Δ^7-Dafachronic Acid

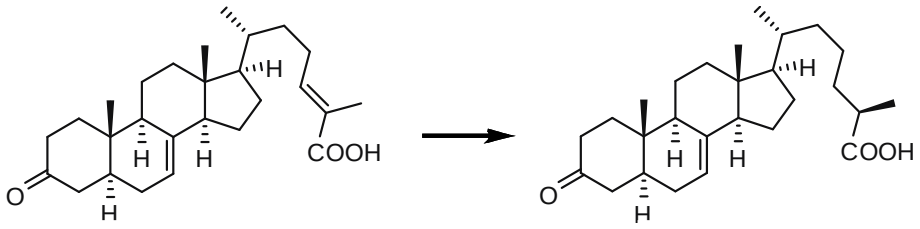

(*E*)-3-keto-5α-cholest-7,24-enoic acid **(25*R*)-Δ^7-DA**

A dry 100 mL Schlenk flask was charged with (*E*)-3-keto-5α-cholest-7,24-enoic acid (25 mg, 0.06 mmol, 1.0 equiv.) (Judkins, J.C., et al. *Angew Chem.*In revision), Teflon®-coated magnetic stir bar, and methanol (10 mL). The flask was equipped with a reflux condenser and while stirring, was flushed with argon for 15 minutes. *(R)*-Ru(OAc)$_2$[H_8-BINAP] (2 mg, 2 μmol, 0.04 equiv.) dissolved in methanol (5 mL) was then added. The reaction flask was warmed to 50 °C

and flushed with a vigorous flow of hydrogen for one minute. The hydrogen flow rate was decreased to a slow and steady rate and the reaction was allowed to stir for three hours. The reaction was concentrated *in vacuo* and flash column chromatography on silica gel using a 0-60% (*v/v*) gradient of ethyl acetate containing 0.25% acetic acid in hexanes afforded (25*R*)-Δ^7-dafachronic acid. (14.2 mg, 0.034 mmol, 60%) as a white solid. NMR and optical rotation data matched those reported previously (Giroux and Corey, 2008).

(25*S*)-$\Delta^{1,7}$-Dafachronic Acid

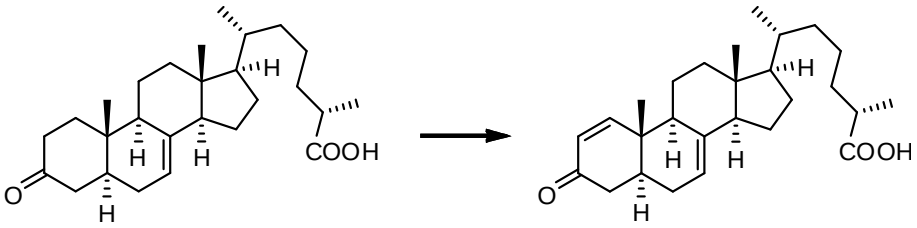

(25*S*)-Δ^7-DA **(25*S*)-$\Delta^{1,7}$-DA**

To a dry 20 mL scintillation vial was added (25*S*)-Δ^7-dafachronic acid (22 mg, 0.05 mmol, 1.0 equiv.), Teflon®-coated magnetic stir bar, 2-iodoxybenzoic acid (46 mg, 0.16 mmol, 3.0 equiv.), DMSO (5 mL), and trifluoroacetic acid (1.2 μL, 16 μmol, 0.3 equiv.). The reaction mixture was stirred at 70 °C for two days. The reaction was cooled to room temperature and water (10 mL) was slowly added. The water-DMSO layer was extracted three times with ethyl acetate (5 mL) and the combined ethyl acetate layers were dried over Na_2SO_4 and concentrated *in vacuo*. The yellowish solid was purified by flash column chromatography on silica gel using a 0-60% (*v/v*) gradient of ethyl acetate containing 0.25% acetic acid in hexanes afforded (25*S*)-$\Delta^{1,7}$-dafachronic acid (17 mg, 0.042 mmol, 85%) as a white crystalline solid. α_D^{20}= +21.1. HRMS *m/z* $[C_{27}H_{39}O_3]^-$ = 411.2905 (expected); HRMS *m/z* $[C_{27}H_{39}O_3]^-$ = 411.2873, **(Table S1)**.

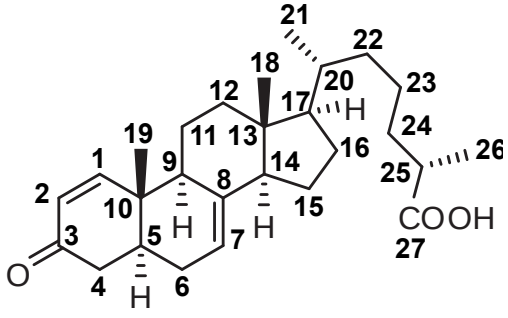

$\Delta^{1,7}$-dafachronic acid

(25*R*)-$\Delta^{1,7}$-Dafachronic Acid

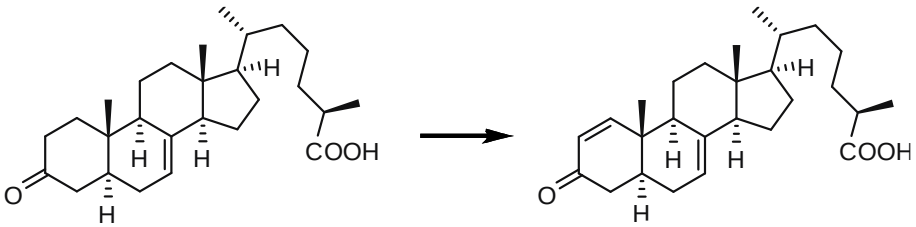

(25*R*)-Δ^{7}-DA **(25*R*)-$\Delta^{1,7}$-DA**

(25*R*)-Δ^{7}-dafachronic acid (20 mg, 0.05 mmol, 1.0 equiv.) was dissolved in Et_2O (1 mL) in an 8 mL scintillation vial and a Teflon®-coated magnetic stir bar added. The reaction mixture was stirred very vigorously while a solution of HBr in acetic acid (8.6 mg of 9.84 mg/100 μL solution, 10 μmol, 0.2 equiv.) was added. A solution of Br_2 in acetic acid (140 mg of 62.8 mg/1 mL solution, 0.05 mmol, 1.05 equiv.) was added in two portions and the reaction allowed to stir for 10 minutes. The reaction was quenched by the addition of saturated $NaHCO_3$ (0.3 mL), 50% saturated NaCl (1.0 mL), and $KHSO_4$ (300 mg). The reaction mixture was then extracted with Et_2O (three 1 mL portions), the Et_2O layers dried over $MgSO_4$, and concentrated *in vacuo*. Flash column chromatography on silica gel using a 0-60% (*v/v*) gradient of ethyl acetate containing 0.25% acetic acid in hexanes afforded (25*R*)-2-bromo-Δ^{7}-dafachronic acid (7.6 mg, 0.015 mmol, 31%) as a white solid. (25*R*)-2-bromo-Δ^{7}-dafachronic acid (7.6 mg, 0.015 mmol, 1.0 equiv.) was suspended in DMF (200 μL) and LiBr (15.4 mg, 0.18 mmol, 11.5 equiv.) and Li_2CO_3 (28.4 mg, 0.39 mmol, 25 equiv.) were then added and heated at 150 °C for 10 minutes. Flash column chromatography on silica gel using a 0-60% (*v/v*) gradient of ethyl acetate containing 0.25% acetic acid in hexanes afforded (25*R*)-$\Delta^{1,7}$-dafachronic acid (1.3 mg, 0.003 mmol, 21%) as a white solid. ^{1}H NMR (600 MHz, $CDCl_3$) δ (ppm) 0.57 (s, 3H), 0.93 (d, 3H, J = 6.6 Hz), 0.95 (s, 3H), 0.98-1.16 (m 2H), 1.19 (d, 3H, J = 7 Hz), 1.22-1.24 (m, 1H), 1.28-1.48 (m, 3H), 1.49-1.95 (m, 14H), 2.38-2.64 (m, 2H), 2.48 (sext., 1H, J = 6.8 Hz), 5.26 (bs, 1H), 5.90 (d, 1H, J = 10.2 Hz), 7.01 (d, 1H, J = 10.2 Hz). ^{13}C NMR (125 MHz, $CDCl_3$) δ (ppm) 11.9, 12.6, 16.8, 18.7, 21.6, 22.8, 27.7, 27.9, 28.5, 29.6, 33.9, 34.1, 35.7, 38.7, 39.3, 39.6, 40.1, 43.5, 45.2, 55.1, 55.9, 117.8, 127.1, 138.8, 157.3, 179.1, 200.0. α_D^{20}= +10.5. HRMS *m/z* $[C_{27}H_{39}O_3]^-$ = 411.2905 (expected); HRMS *m/z* $[C_{27}H_{39}O_3]^-$ = 411.2911.

(25*S*)-5α-Δ^0-Dafachronic Acid

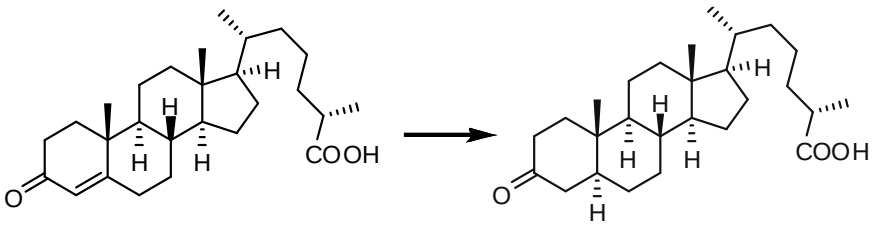

(25*S*)-Δ^4-DA **(25*S*)-Δ^0-DA**

The middle neck of a dry three-neck 50 mL round-bottomed flask charged with a Teflon®-coated magnetic stir bar was equipped with a dry ice-acetone condenser, one side neck was equipped with a valve and the final neck was equipped with a rubber stopper. An argon inlet was attached to the valve and a mineral oil bubbler attached to the outlet from the dry ice-acetone condenser. After flushing the system with argon for approximately 15 minutes, the flask was charged with lithium (13.3 mg, 1.92 mmol, 5 equiv.) and the argon inlet was exchanged for an ammonia line. After a positive flow of ammonia gas was established, the flask was submerged in a dry ice-acetone bath and the condenser was charged with dry ice and acetone. After approximately 10 mL ammonia had condensed, the input gas was quickly exchanged for an argon inlet with a slow but steady stream of argon. After 45 minutes of rapid stirring, a solution of (25*S*)-Δ^4-dafachronic acid (Motola et al., 2006) (0.159 g, 0.38 mmol, 1.0 equiv.), *t*-butanol (0.2 mL, 2.1 mmol, 5.1 equiv.), and freshly distilled tetrahydrofuran (10 mL) was added slowly via syringe through the rubber septum. After addition was complete, the reaction was maintained at -78 °C for one hour and was then quenched with NH_4Cl. The dry ice-acetone condenser and bath were removed and the ammonia was allowed to evaporate. When evaporation was complete, water (10 mL) was added to the resultant off-white chunky mixture, and the mixture was acidified with acetic acid and extracted three times with dichloromethane (10 mL portions). The combined dichloromethane extracts were then dried with Na_2SO_4 and concentrated *in vacuo*. Flash column chromatography on silica gel using a 0-60% (*v/v*) gradient of ethyl acetate containing 0.25% acetic acid in hexanes afforded (25*S*)-5α-Δ^0-dafachronic acid (0.144 g, 0.35 mmol, 90%) as a white crystalline solid. NMR spectroscopic and optical rotation data of the product was identical to those reported previously (Martin et al., 2008).

3α-OH-(25*S*)-Δ^7-Dafachronic Acid

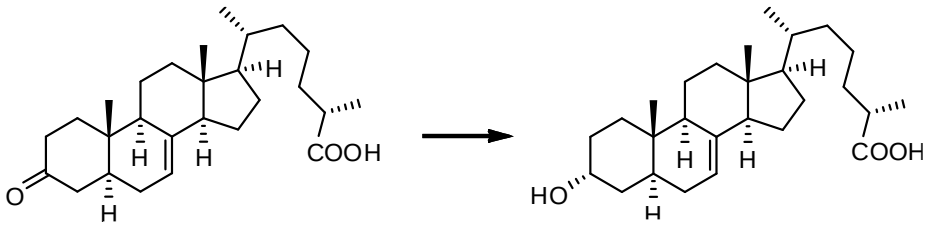

(25*S*)-Δ^7-DA **3α-OH-Δ^7-DA**

To a dry 8 mL vial was added (25*S*)-Δ^7-dafachronic acid (0.4 mg, 0.96 μmol, 1.0 equiv.), Teflon®-coated magnetic stir bar, and THF (0.5 mL). The reaction was cooled to -78 °C and K-selectride® (1.0 M solution in THF, 0.2 μL, 0.2 μmol, 2.2 equiv.) was then added drop-wise and the reaction stirred at room temperature for 90 min. Subsequently, the reaction was acidified with 1N HCl and concentrated *in vacuo*. The white crude residue was resuspended in 1 mL H_2O and extracted three times with ethyl acetate, the ethyl acetate layers were dried over Na_2SO_4 and concentrated *in vacuo*. The white solid was purified by flash column chromatography on silica gel using a 0–60% (*v/v*) gradient of ethyl acetate containing 0.25% acetic acid in hexanes to afford 3α-OH-(25*S*)-Δ^7-dafachronic acid (350 μg, 0.8 μmol, 87%) as a white solid. α_D^{20}= +8.7. HRMS *m/z* $[C_{27}H_{43}O_3]^-$ = 415.3218 (expected) HRMS *m/z* $[C_{27}H_{43}O_3]^-$ = 415.3253, **(Table S2)**.

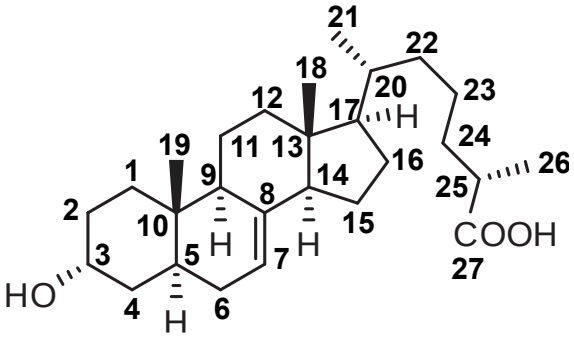

3α-OH-Δ^7-dafachronic acid

3β-OH-(25*S*)-Δ^7-Dafachronic Acid

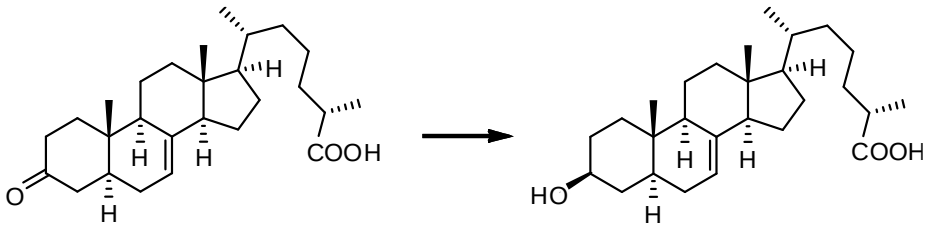

(25*S*)-Δ^7-DA **3β-OH-Δ^7-DA**

To a dry 8 mL vial was added (25*S*)-Δ^7-dafachronic acid (0.6 mg, 1.4 μmol, 1.0 equiv.), Teflon®-coated magnetic stir bar, and EtOH (0.25 mL). $NaBH_4$ (0.1 mg, 2.9 μmol, 2.0 equiv.) was then added and the reaction stirred at room temperature for 10 minutes. The reaction was acidified with 1N HCl and concentrated *in vacuo*. The white crude residue was resuspended in 1mL H_2O and extracted three times with ethyl acetate, the ethyl acetate layers were dried over Na_2SO_4 and concentrated *in vacuo*. The white solid was purified by flash column chromatography on silica gel using a 0-60% (*v/v*) gradient of ethyl acetate containing 0.25% acetic acid in hexanes to afford 3β-OH-(25*S*)-Δ^7-dafachronic acid (260 μg, 0.062 mmol, 43%) as a white solid. ^{1}H NMR (600 MHz, $CDCl_3$) δ (ppm) 0.53 (s, 3H), 0.79 (s, 3H), 0.91 (d, 3H, J = 6.5 Hz), 1.18 (d, 3H, J = 7 Hz), 2.47 (sextet, 1H, J = 7 Hz), 3.54-3.66 (m, 1H), 5.2 (bs, 1H). ^{13}C NMR (151 MHz, $CDCl_3$) δ (ppm) 12.0, 13.2, 17.2, 18.9, 21.7, 23.1, 23.9, 28.1, 29.8, 31.6, 34.2, 34.3, 35.9, 36.2, 37.3, 38.1, 39.3, 39.7, 40.4, 43.5, 49.6, 55.2, 56.2, 71.2, 117.4, 139.7, 179.2. α_D^{20}= +6.3. HRMS *m/z* $[C_{27}H_{43}O_3]^-$ = 415.3218 (expected) HRMS *m/z* $[C_{27}H_{43}O_3]^-$ = 415.3211.

NMR Spectra of Synthetic Compounds

^{1}H NMR Spectrum (600 MHz, $CDCl_3$) of (25*S*)-$\Delta^{1,7}$-Dafachronic Acid

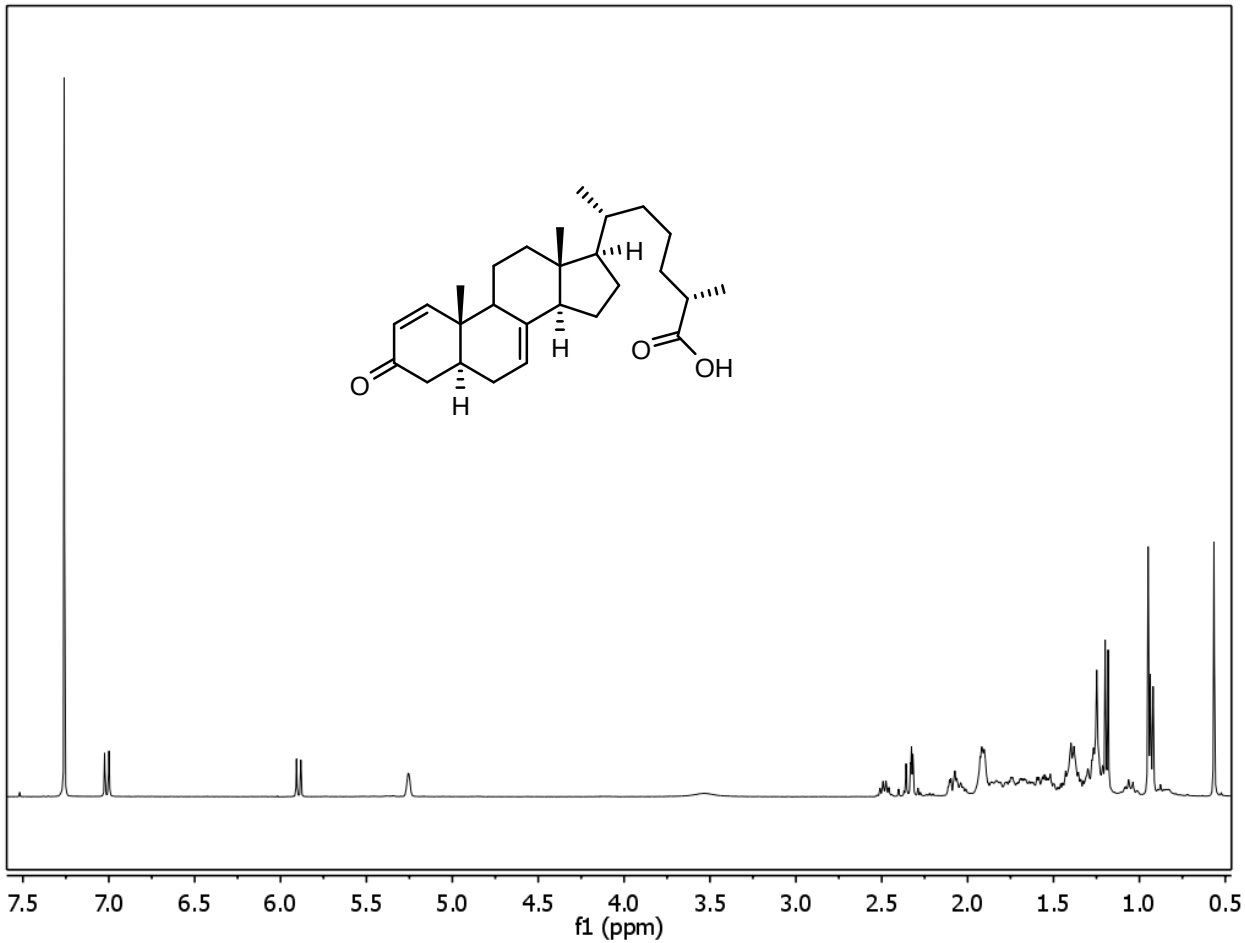

dqfCOSY Spectrum (600 MHz, $CDCl_3$) of (25*S*)-$\Delta^{1,7}$-Dafachronic Acid

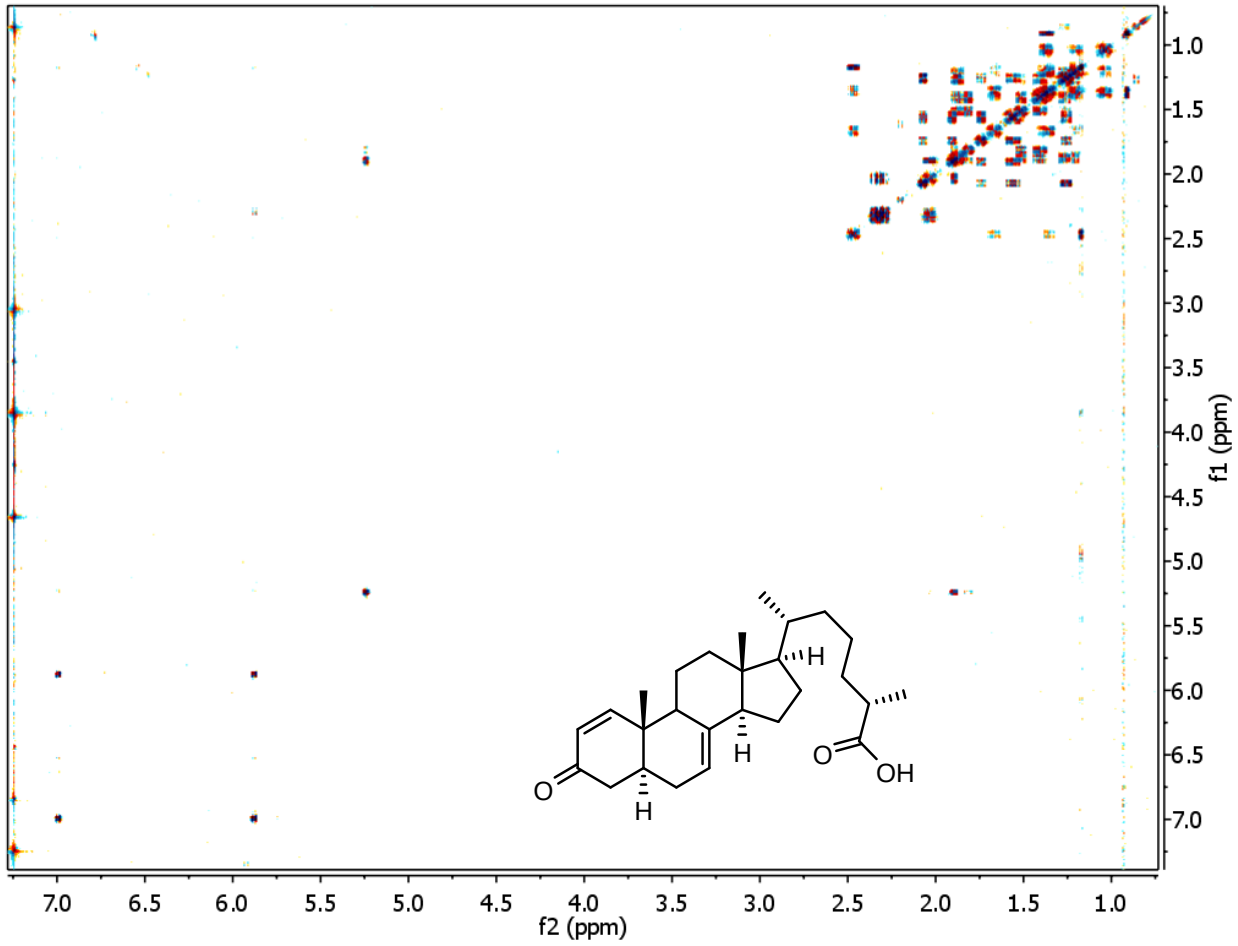

HMQC Spectrum (600 MHz for ^{1}H, 151 MHz for ^{13}C, $CDCl_3$) of (25*S*)-$\Delta^{1,7}$-Dafachronic Acid

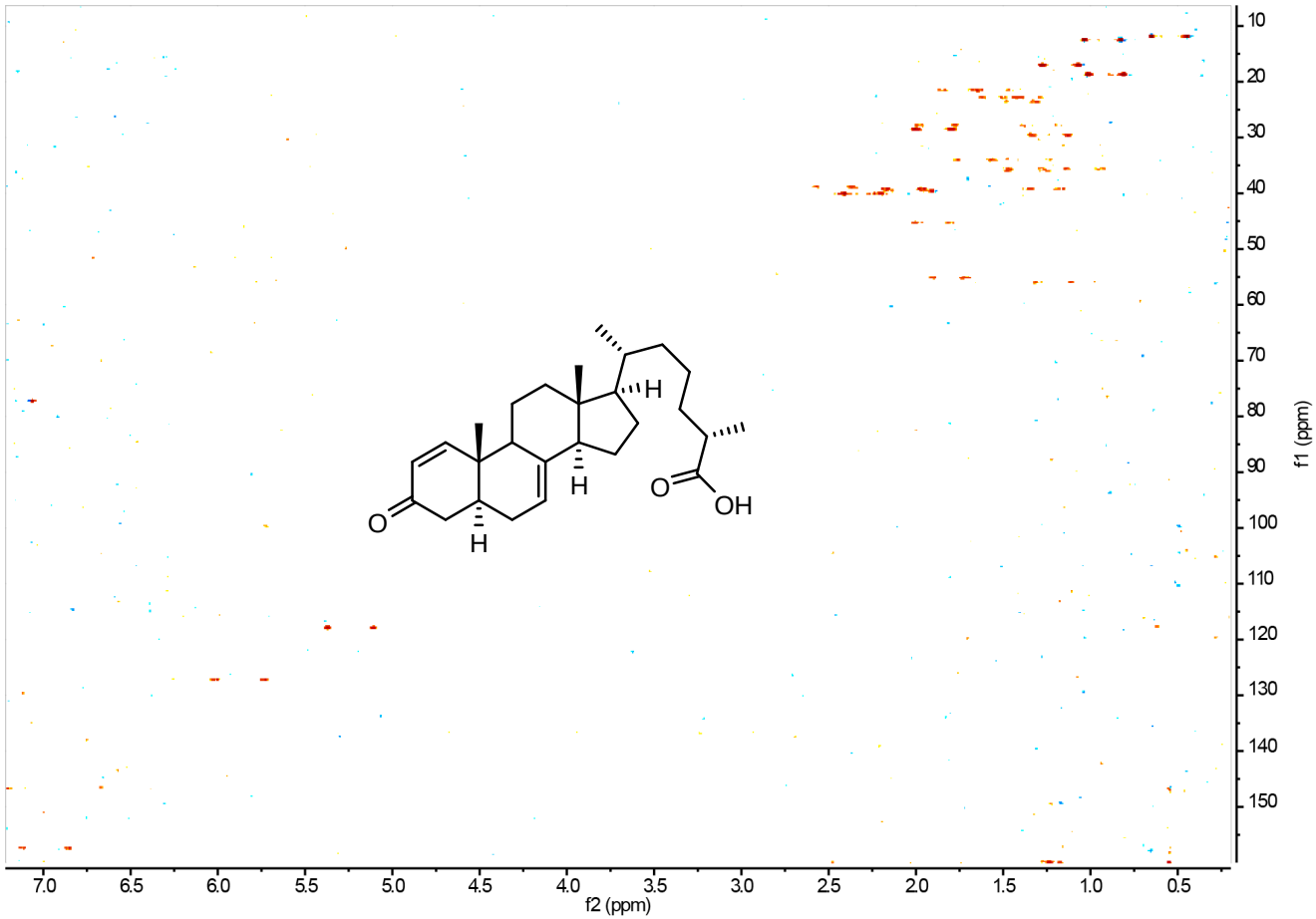

HMBC Spectrum (600 MHz for ^{1}H, 151 MHz for ^{13}C, $CDCl_3$) of (25*S*)-$\Delta^{1,7}$-Dafachronic Acid

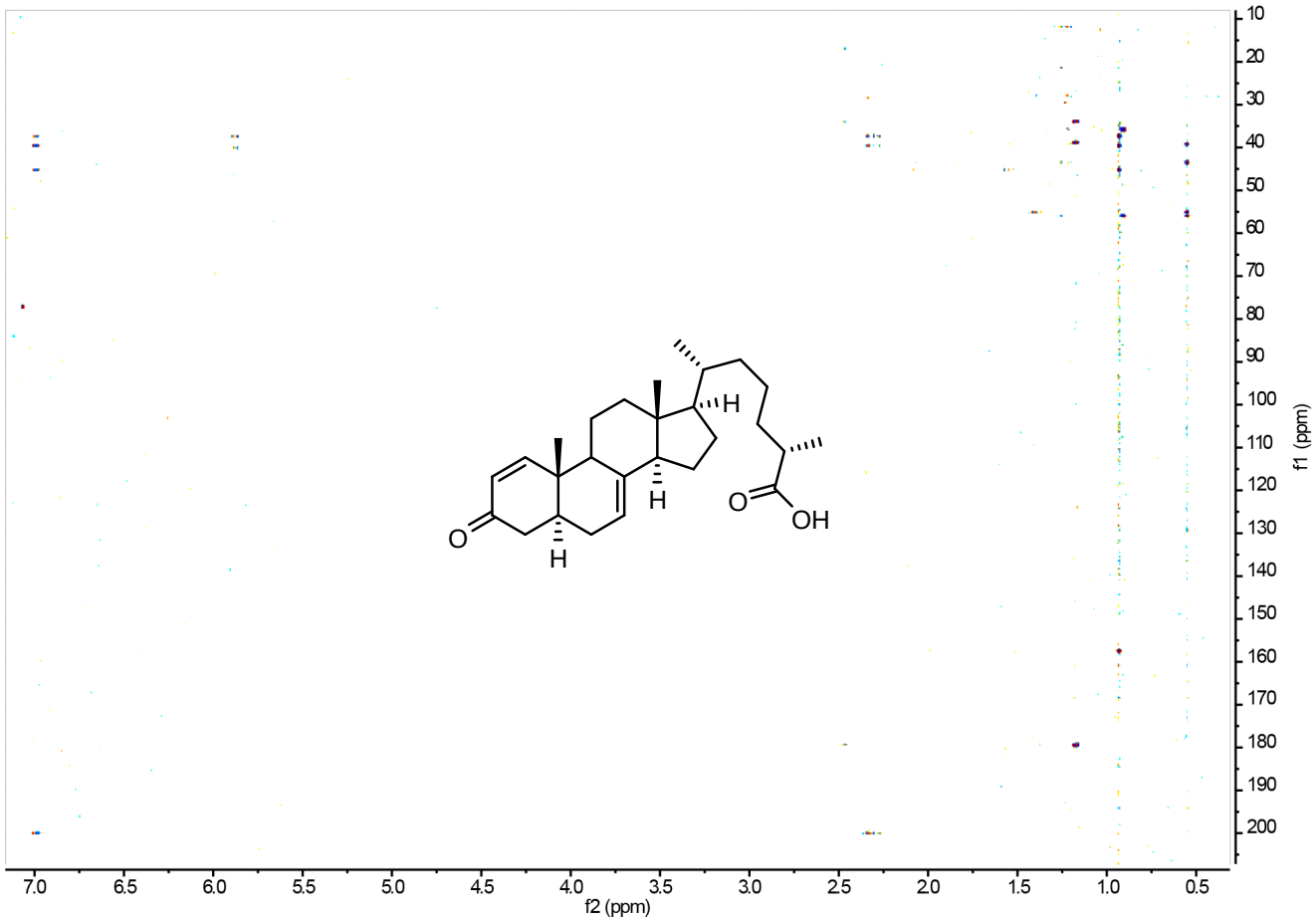

^{1}H NMR Spectrum (600 MHz, $CDCl_3$) of 3α-OH-(25*S*)-Δ^7-Dafachronic Acid

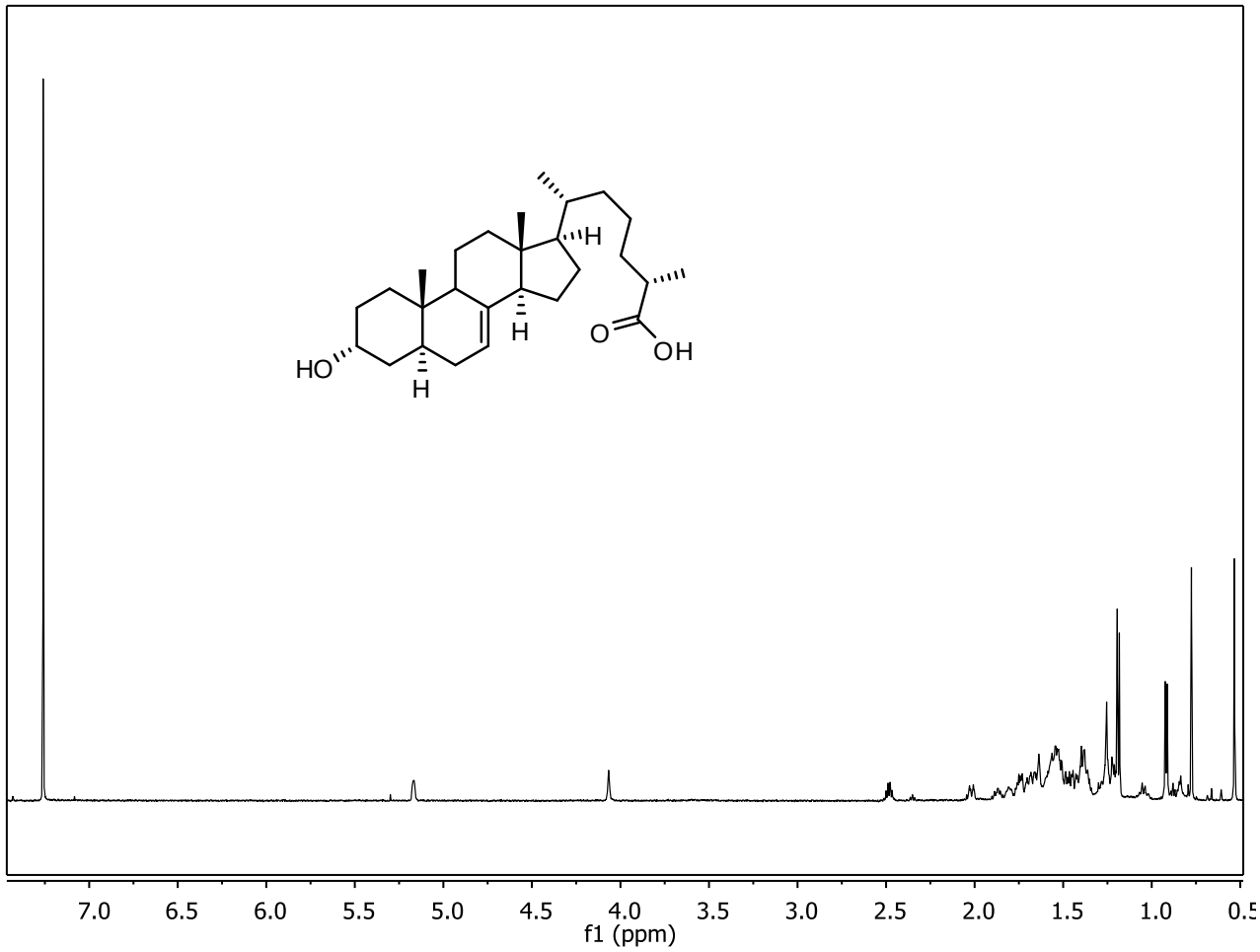

dqfCOSY Spectrum (600 MHz, $CDCl_3$) of 3α-OH-(25*S*)-Δ^7-Dafachronic Acid

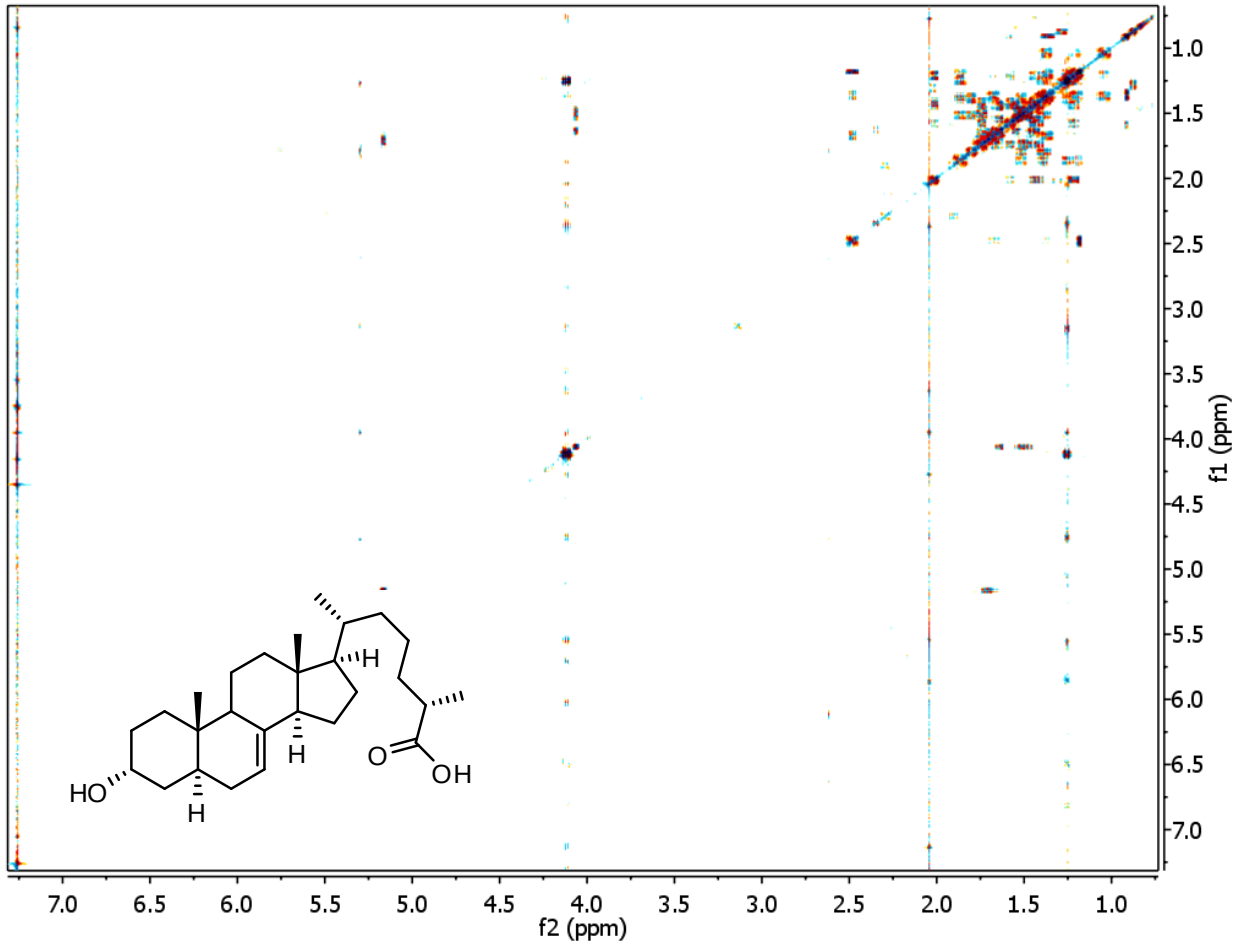

HMQC Spectrum (600 MHz for ^{1}H, 151 MHz for ^{13}C, $CDCl_3$) of 3α-OH-(25*S*)-Δ^7-Dafachronic Acid

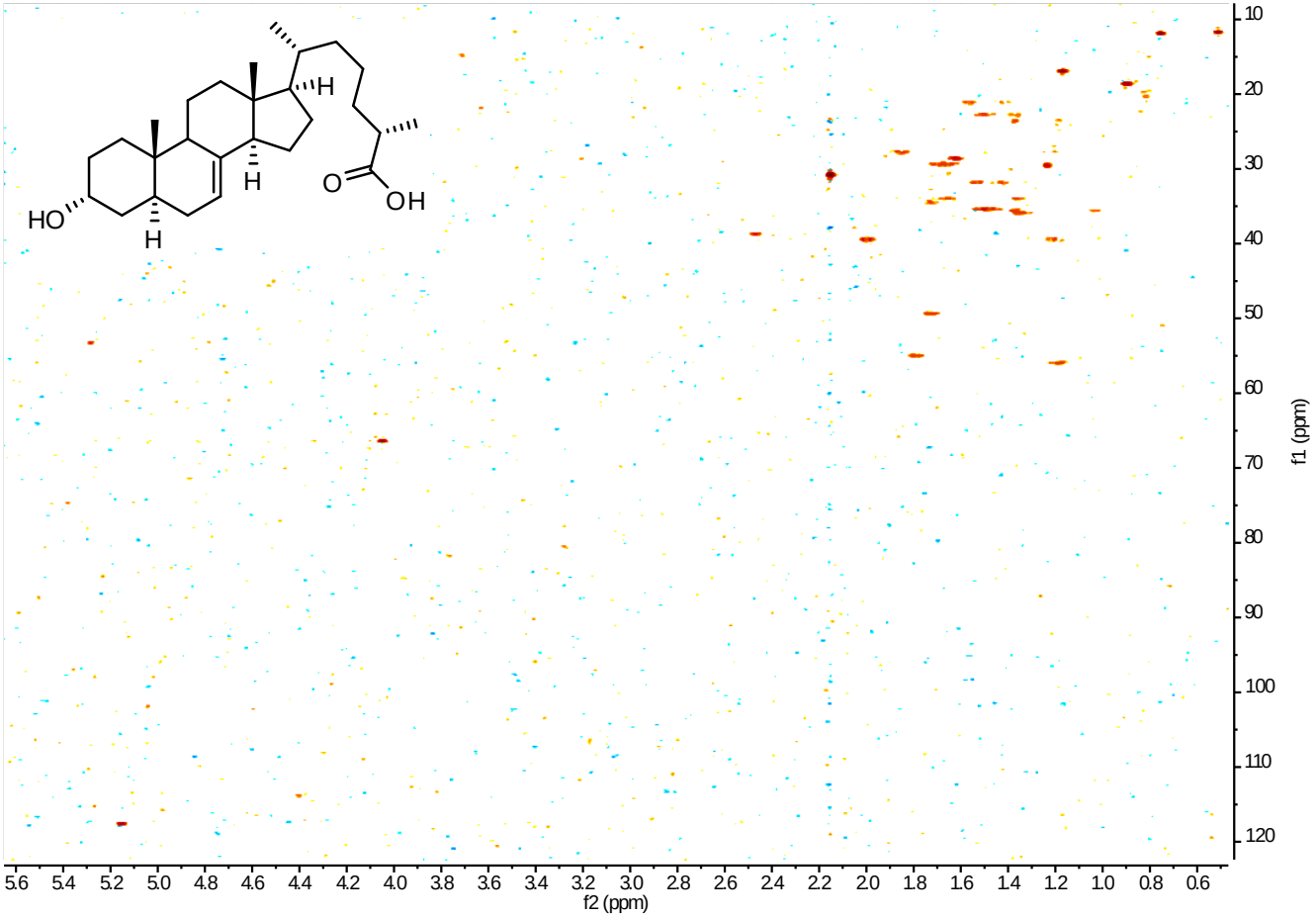

HMBC Spectrum (600 MHz for ^{1}H, 151 MHz for ^{13}C, $CDCl_3$) of 3α-OH-(25*S*)-Δ^{7}-Dafachronic Acid

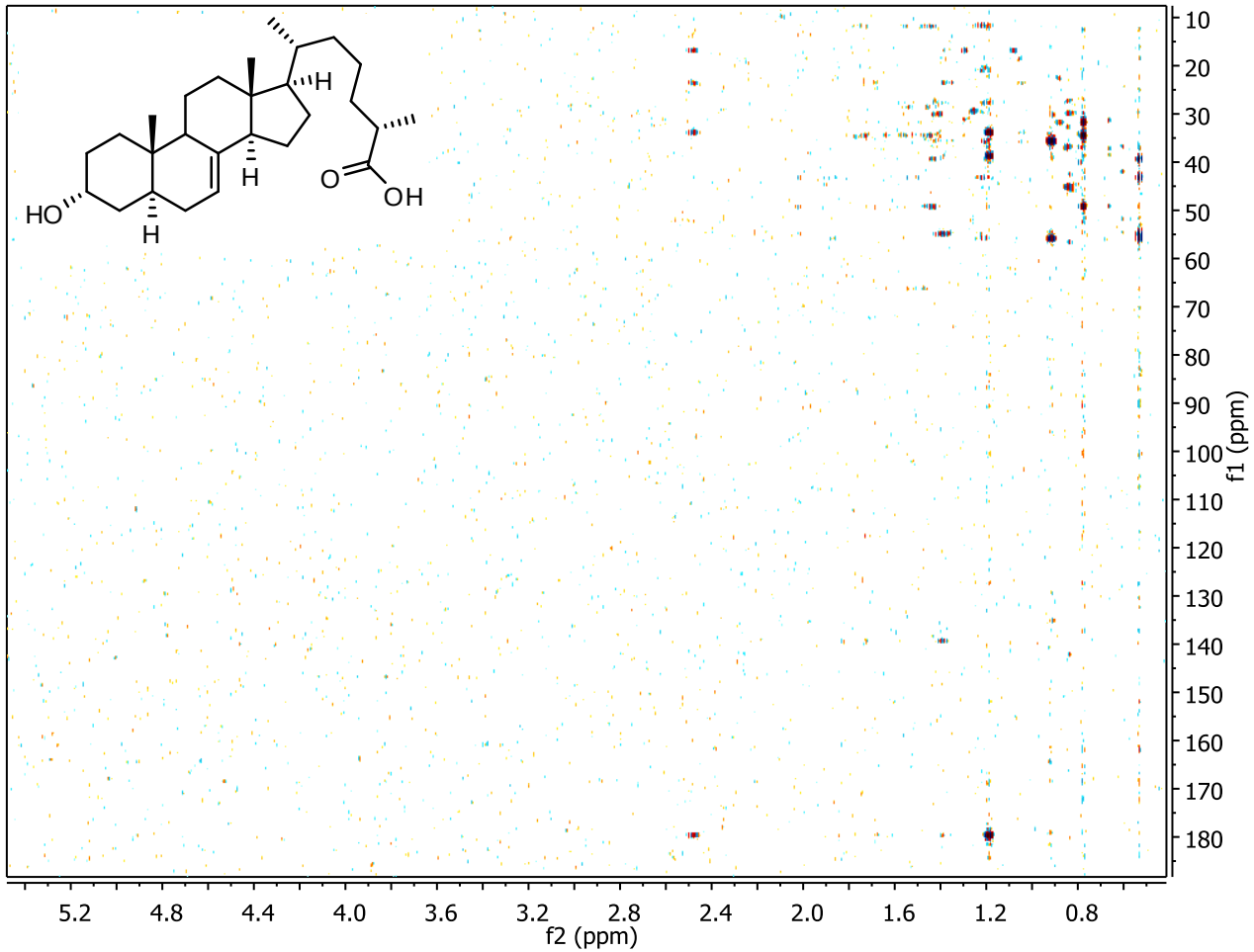

^{1}H NMR Spectrum (600 MHz, $CDCl_3$) of 3β-OH-(25*S*)-Δ^7-Dafachronic Acid

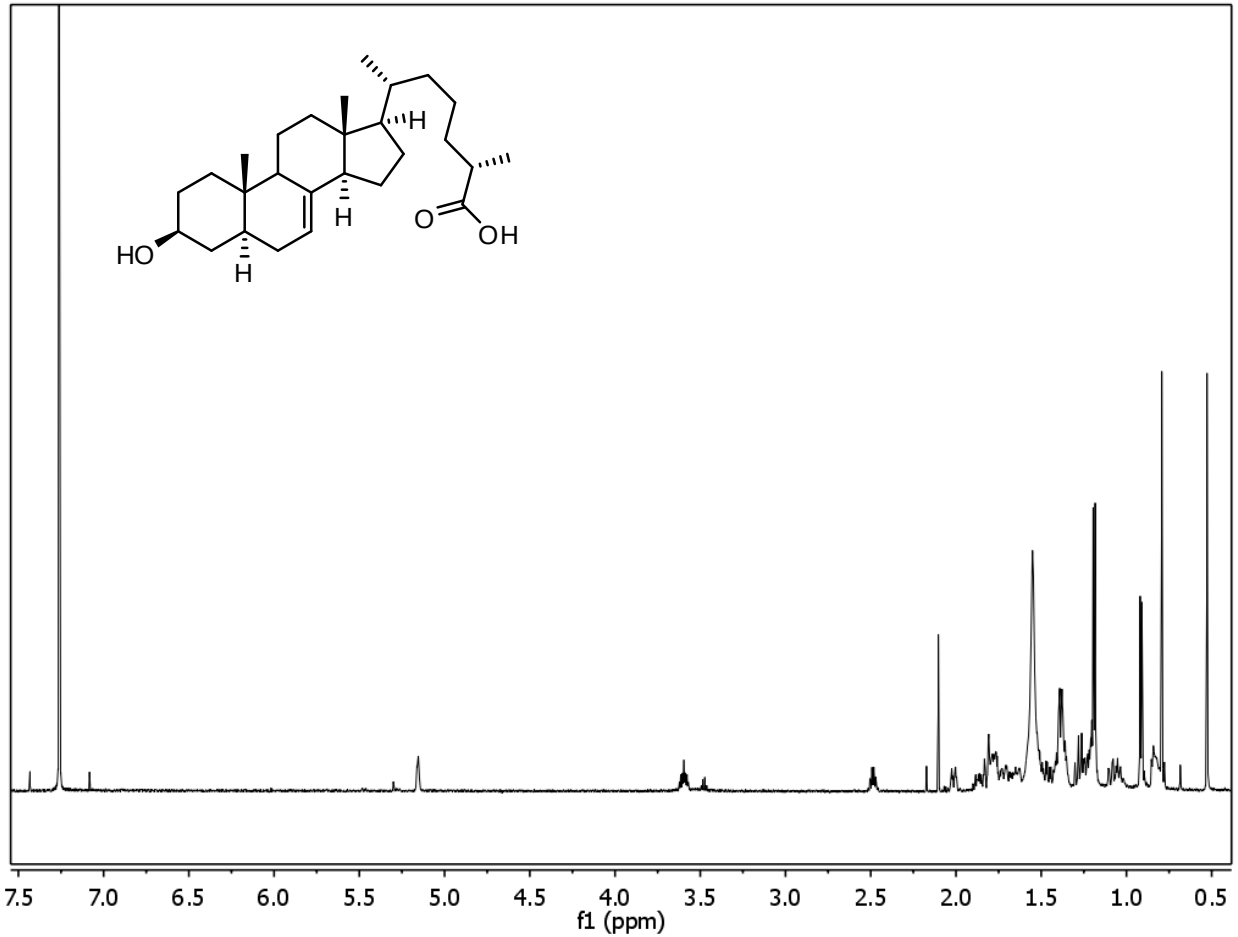

dqfCOSY Spectrum (600 MHz, $CDCl_3$) of 3β-OH-(25*S*)-Δ^7-Dafachronic Acid

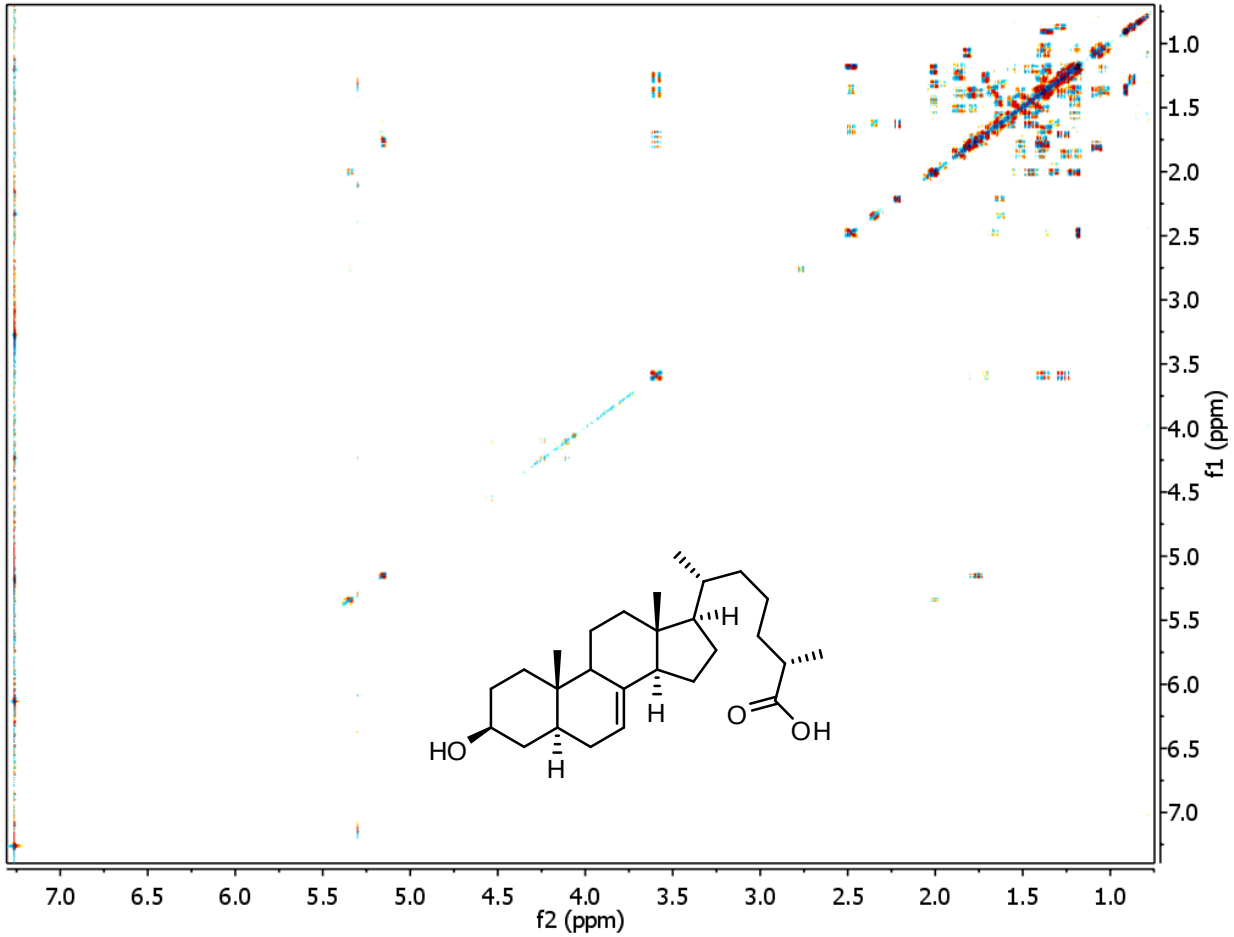

SUPPLEMENTAL REFERENCES

Giroux, S., and Corey, E.J. (2007). Stereocontrolled synthesis of dafachronic acid A, the ligand for the DAF-12 nuclear receptor of Caenorhabditis elegans. J Am Chem Soc *129*, 9866-9867. Epub 2007 Jul 9821.

Giroux, S., and Corey, E.J. (2008). An efficient, stereocontrolled synthesis of the 25-(R)-diastereomer of dafachronic acid A from beta-ergosterol. Org Lett *10*, 801-802.

Gunatilaka, A.A.L., Gopichand, Y., Schmitz, F.J., and Djerassi, C. (1981). Minor and trace sterols in marine-invertebrates .26. Isolation and structure elucidation of 9 new 5-alpha,8-alpha-epidioxy sterols from 4 marine organisms. J Org Chem *46*, 3860-3866.

Held, J.M., White, M.P., Fisher, A.L., Gibson, B.W., Lithgow, G.J., and Gill, M.S. (2006). DAF-12-dependent rescue of dauer formation in Caenorhabditis elegans by (25S)-cholestenoic acid. Aging Cell *5*, 283-291.

Martin, R., Dabritz, F., Entchev, E.V., Kurzchalia, T.V., and Knolker, H.J. (2008). Stereoselective synthesis of the hormonally active (25S)-delta7-dafachronic acid, (25S)-Delta4-dafachronic acid, (25S)-dafachronic acid, and (25S)-cholestenoic acid. Org Biomol Chem *6*, 4293-4295.

Motola, D.L., Cummins, C.L., Rottiers, V., Sharma, K.K., Li, T.T., Li, Y., Suino-Powell, K., Xu, H.E., Auchus, R.J., Antebi, A., *et al.* (2006). Identification of ligands for DAF-12 that govern dauer formation and reproduction in C. elegans. Cell *124*, 1209-1223.

Yaoita, Y., Amemiya, K., Ohnuma, H., Furumura, K., Masaki, A., Matsuki, T., and Kikuchi, M. (1998). Sterol constituents from five edible mushrooms - Part III. Chem Pharm Bull *46*, 944-950.